Optimal Design of Wheelchair Drive Mechanism

Perwez Akhtar
Karthik Reddy Kothakota
Vishwesh Nampurkar
Clare McNamara
ME 555-2011-12

Winter 2011 Report

The standard manual wheelchair requires a great deal of force to propel forward using a back to front motion. The efficiency of driving the wheelchair forward may be increased by adding a ratchet and pawl type drive mechanism to the wheel, allowing for the passenger to apply force in a pulling motion. The objective of the optimization of the overall system is to minimize the force required to drive the wheelchair forward. The drive mechanism system can be broken down into four sub systems, each to be optimized individually: the lever handle, the gears, the shaft, and the wheel. The lever handle has been optimized in order to maximize the work done by the lever through a given angle. The gears have been optimized in order to minimize the volume and maximize the fatigue life. The shaft has been optimized in order to minimize their volume. The wheel has been optimized in order to minimize its mass. The subsystems were then integrated and the entire system of the drive mechanism was optimized for the maximum work output. The links and tradeoffs between the subsystems cause the values of the overall optimization to be different than the optimum values of the subsystems.

Contents

1. Introduction

A majority of the mobility solutions for disabled individuals involve wheelchairs with a hand drive mechanism. This mechanism involves fixing a rim to the wheel, whose diameter is slightly less than that of the wheel. It is well known that this kind of design causes discomfort for the occupant, possibly leading even to dislocation of shoulders (1) (2). There have been several attempts to increase the efficiency of such systems by reducing the amount of effort required to drive such mechanisms. This project looks at one such mechanism and deals with the optimization of the design of this new mechanism in order to minimize the effort required to drive and maximize the torque output.

To better understand the system and its various components, it is necessary to explain the mechanism first. This new drive mechanism consists of a hand lever, a ratchet and pawl, a gear system and the wheel, connected by two shafts. The lever rotates through an angle to propel the wheelchair forward. The lever is connected to the axle of the wheel through a ratchet and pawl and internal gears. The ratchet and pawl ensure the force is transmitted only in one direction and in the other direction the wheel rotates free. This is very similar to a torque wrench. The ratchet and pawl is attached to the mechanism at the base of the lever. The lever rotates about a pivot which lies at the base of the handle. When the user pulls the handle of the lever, the pawl engages with the teeth of the ratchet (backward curved), thereby driving it forward. When the user moves the handle back to its initial position in the front, the spring loaded pawl just bumps over the revolving ratchet's backward curved teeth.

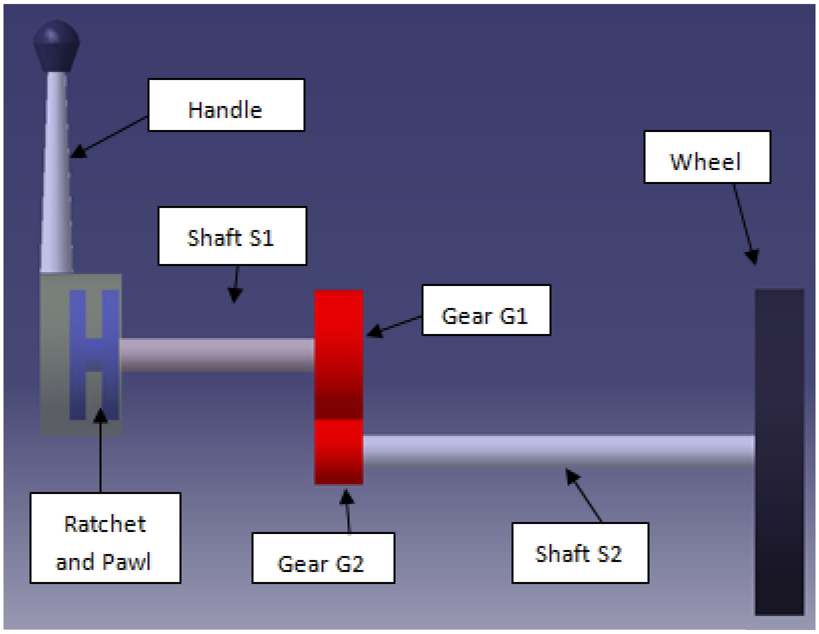

Figure 1: Schematic of the wheelchair drive system to be optimized.

Mechanical advantage is achieved by incorporating a gear system between the ratchet and pawl mechanism, and the stub axle of the wheelchair. The output of the rotating ratchet is given to a gear G1 through a shaft S1. G1 then meshes with another gear G2 which is present on the shaft S2, to transmit the final torque to the wheels.

The objective of this optimization project is to maximize the work done by the lever for a given stroke angle without causing discomfort to the user. Because the subsystems of this drive mechanism physically link together, and the forces will be transmitted throughout the different subsystems (the handle, the shafts, the gears, and the wheel), and because the entire system must meet the packaging standards of the current manual wheelchair design, there will be tradeoffs between these subsystems. The sizes of each subsystem component will impact the sizes of the others. Additionally, all the components will have to meet packaging constraints together, so there will be tradeoffs in order to meet the packaging demands. The expected tradeoffs between the subsystems include volume of each different subsystem versus the others, and transmission of forces versus losses between the subsystems. Because the subsystems also need to meet strength constraints, it is expected that their independent optimizations will not lead to an overall optimal system.

2 Handle Lever – Perwez Akhtar

2.1 Problem Statement

The objective of this subsystem is to maximize the work done for revolving the crank lever through a given angle. To propel the wheelchair the handle lever will be rotated about the wheel axis to transmit torque to the transmission system. Since the lever comes in direct contact with the occupant the major emphasis in this subsystem is the ergonomics between the occupant/chair interfaces, this project is concerned with the optimization of the crank location with respect to the wheelchair occupant.

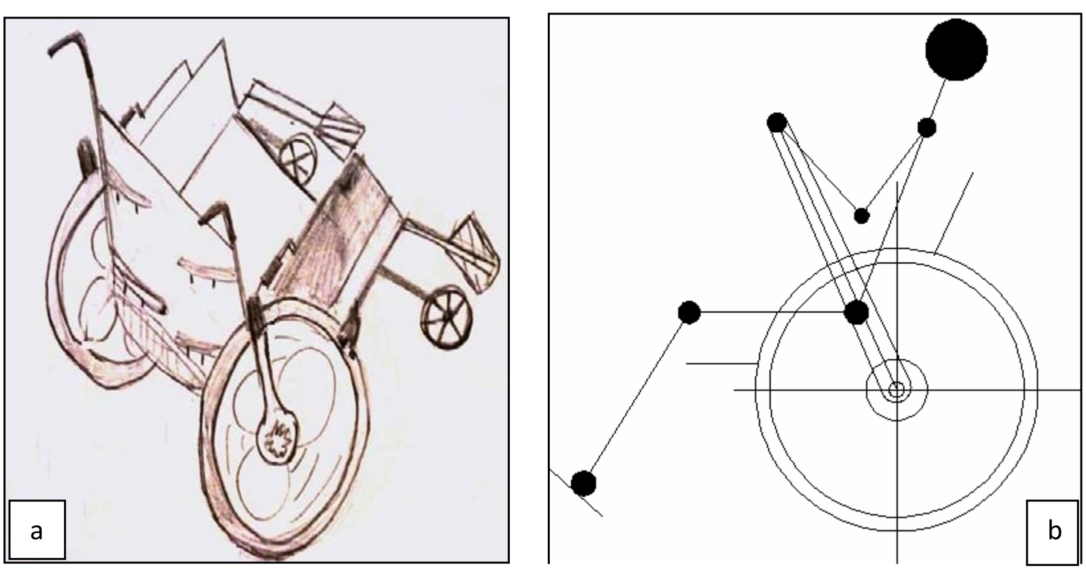

Figure 1: a) Schematic of wheelchair with drive mechanism attached to wheel. **b)** Side view schematic of wheelchair user, lever and wheel.

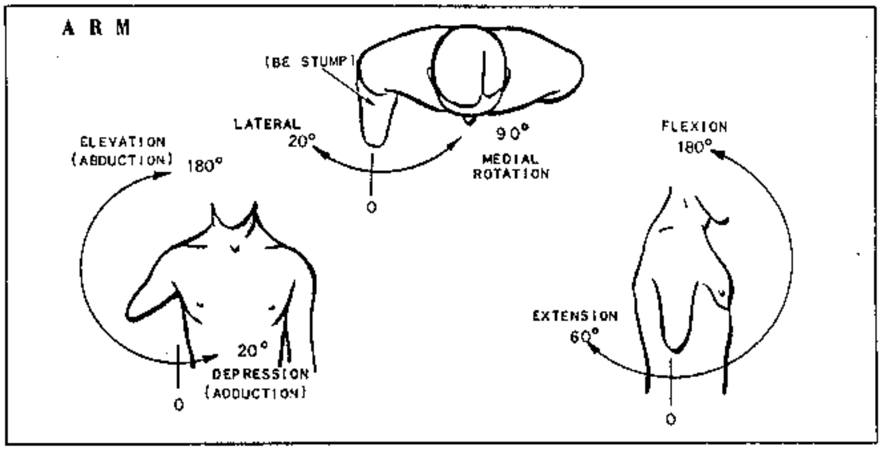

Figure 2: Diagram of range of motion of human arm

Figure 2 shows various body configurations which are dependent upon the angles of the limbs. We see that depression and elevation and flexion and extension will be the two types of configuration that the body will attain when using the crank lever drive mechanism.

For the design to be practical the system should be such that the occupant may operate it for extended periods of time without fatiguing. In using upper body motion as is required by the drive mechanism the shoulder is usually the first joint to tire. This is primarily due to the fact that the shoulder socket is supported entirely by muscles and must support the shoulder in rotation about two dimensions rather than one. Therefore the amount of shoulder rotation will be considered (3) (4).

2.2 Nomenclature

Symbol	**Description**	**Units**
R	Length of the lever	m
T	Torque at crank end	Nm
X	Horizontal distance from shoulder to crank	m
Y	Vertical distance from shoulder to crank	m
Θ_1	Shoulder Angle	Radians
Θ_2	Elbow Angle	Radians

Θ_3	Crank Angle	Radians
L_1	Shoulder length	m
L_2	Elbow length	m
M_1	Mass of shoulder	kg
M_2	Mass of elbow	kg
α_1	Correction Factor for shoulder torque equation	
α_2	Correction Factor for elbow torque equation	
Θ	Angle of revolution of the crank	Radians
T	Torque at crank end	Nm
R_{wheel}	Radius of wheel	m
g	Acceleration due to Gravity	m/s^2
W	Work done to rotate the crank through an angle Θ	Nm
S_h	Shoulder height in seated position	m

2.3 Mathematical Model

2.3.1 Objective function

To model the system we consider that the shoulder undergoes only 1° of freedom, flexion and extension and neglect the depression and elevation mode. Under this simplification the system can be modeled as a planar 4 bar link mechanism with the occupant shoulder and crank center acting as ground (5).

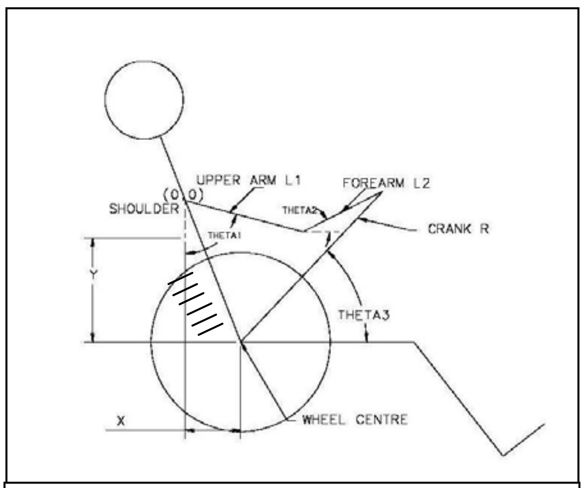

Figure 3: Diagram of relationship between arm and lever

The torque will be dependent upon angle through which the shoulder moves (Θ_1) and the angle through which the elbow moves (Θ_2).This project tries to optimize the position of the lever (X) and its length (R) for maximum work output. The initial orientation of the lever is fixed at 60^0 and the stroke angle is fixed as 60^0. The crank is fixed to the centre of the wheel thus the vertical distance of the shoulder to the crank(Y) is also fixed.

Work done when the crank moves through an angle $d\theta_3$ is given by:

$$\mathrm{dW} = \mathrm{T}\ \mathrm{d}\theta_3$$

where T is in terms of θ_1 and θ_2 and integrand is in terms of θ_3

The objective function is thus stated as:

$$\text{Max W}=\int_{\pi/3}^{2\pi/3} T d\theta_3$$

for rotation through an angle of 60^0 or $\pi/3$.

$$T = \alpha_1(227.338 + 0.525\theta_2) + \alpha_2(336.29 + 1.544\theta_2 - 0.0085\theta_2^2 - 0.51\theta_1) - (M_1 + M_2)g \sin\theta_1 \frac{L_1}{L_2} - M_2 g \cos(\frac{\pi}{2} + \theta_1 - \theta_2)\frac{L_2}{2}$$

2.3.2 Constraints

The system is subjected to various anthropometric constraints. These constraints deal with the occupants reach and joint limitations. As the arms are modeled as a four bar the system is also subjected to kinematic constraints (3).

Equality Constraints

As the linkage is modeled as a 4 bar mechanism, kinematic analysis can be performed on it by writing the loop equations for a planar 4 bar mechanism. Thus the shoulder angle θ_1 and elbow angle θ_2 can be expressed in terms of crank angle θ_3. For a particular value of R and X and Y, θ_3 is the independent variable that will determine the values of θ_1 and θ_2 and hence the function T. The equality constraint must be satisfied for all values for R, X and Y in the entire search domain.

By conserving link lengths the 2 loop equations are:

(a) In the vertical direction

$$-L_1 \cos\theta_1 + L_2 \sin\theta_2 + R\cos\theta_3 - Y = 0$$

We know that shoulder height in a seated position is equal to the vertical distance from shoulder to crank plus the radius of the wheel, and the shoulder height for this case is 1.05m (2).

$$Y + r_o = 1.05$$

The radius of wheel is taken as a parameter, 0.35 m.

$$-L_1 \cos\theta_1 + L_2 \sin\theta_2 + R\cos\theta_3 - 0.7 = 0$$

(b) In the horizontal direction

$$L_1 \sin\theta_1 + L_2 \cos\theta_2 \;\; R\cos\theta_3 - X = 0$$

Inequality Constraints

1) The values of shoulder angle will be limited by the 2 shoulder locking positions.

$$-60^0 \le \theta_1 \le 180^0$$

$$-\frac{\pi}{3} - \theta_1 \le 0$$

$$\theta_1 - \pi \le 0$$

2) The values of elbow angle will be limited by the 2 elbow locking positions.

$$0^0 \le \theta_2 \le 140^0$$

$$-\theta_2 \le 0$$

$$\theta_2 - \frac{7\pi}{9} \le 0$$

3) As the links break contact and do not complete a full revolution we can reduce the search domain of X, Y and R by using combinations which do not satisfy Grashoff's Criteria or are non-Grashoff Linkages (Grashoff's Criteria states that for one fully rotatable link in a 4 bar mechanism the sum of the longest and shortest links must be less than the sum of the other two links). As none of the link can be fully rotated the mechanism is a non-Grashoff linkage (5).

$$\sqrt{X^2 + Y^2} + L_2 > L_1 + R$$

L_1=32.3 cm for 95 percentile males and L_2=28.7 cm.

$$\sqrt{X^2 + Y^2} + L_2 \geq 1.1L_1 + 1.1R$$

Assuming a factor of 10% due to the thickness of the joints.

$$1.1R + (1.1L_1 - L_2) - \sqrt{X^2 + 0.7^2} \leq 0$$

4) The length of the lever should be greater than the height of the armrest so that the handle does not interfere with the hand of the user. If the lever is below the armrest it will not be comfortable to the user. Also this would cause movement by depression rather than flexion and our model of a planar four bar will fail. The height of the armrest from the center of the wheel is 0.45m (6).

$$0.45 - R \leq 0$$

5) The crank will be attached to the center of the wheel. The position of the wheel can now be determined with respect to the shoulder. The wheel can either be in front of the person or behind the person.

a) Wheel in front of the person: X ≥ 0

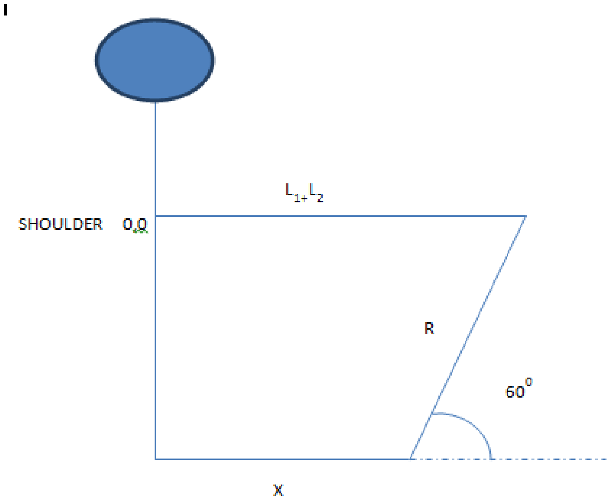

$$-X \leq 0$$

$$X + R\cos\frac{\pi}{3} - (L_1 + L_2) \leq 0$$

Figure 5: Wheel position in front of shoulder

b) Wheel behind the person: X ≤ 0

$$X \leq 0$$

$$-X - R\cos\frac{2\pi}{3} - (L_1 + L_2)\cos\frac{\pi}{3} \leq 0$$

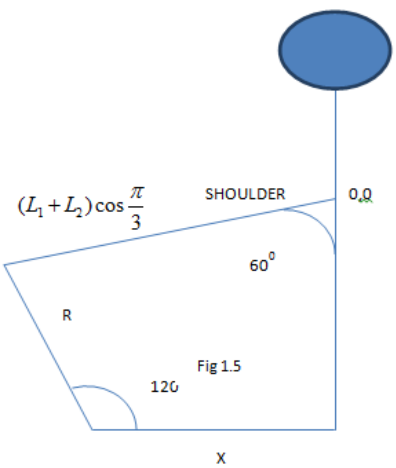

Figure 6: Wheel position behind shoulder

2.3.3 Design Variables

R – Length of the crank lever

X – Horizontal position of the wheel with respect to the shoulder pivot

θ_1 - Shoulder angle

θ_2 - Elbow Angle

2.3.4 System Parameters

L_1 – Length of the shoulder Arm

L_2 – Length of the elbow arm

M_1 - Mass of the shoulder Arm

M_2 - Mass of the elbow arm

α_1 , α_2 - correction factor

2.3.5 Summary

Objective Function

$$\min W = -\int_{\frac{\pi}{3}}^{\frac{2\pi}{3}} \Big[\alpha_1(277.338 + 0.525\theta_2 - 0.296\theta_1) + \alpha_2(336.29 + 1.544\theta_2 - 0.0085\theta_2^2 - 0.5\theta_1) - (M_1 + M_2)g \sin\theta_1 \frac{L_1}{2} - M_2 g \cos\left(\frac{\pi}{2} + \theta_1 - \theta_2\right)\frac{L_2}{2}\Big] d\theta_3$$

Subject to constraints:

h1: $-L_1 \cos\theta_1 + L_2 \sin\theta_2 + R\cos\theta_3 - 0.7 = 0$

h2: $L_1 \sin\theta_1 + L_2 \cos\theta_2 \;\; R\cos\theta_3 - X = 0$

g1: $-\frac{\pi}{3} - \theta_1 \leq 0$

g2: $\theta_1 - \pi \leq 0$

g3: $-\theta_2 \leq 0$

g4: $\theta_2 - \frac{7\pi}{9} \leq 0$

g5: $1.1R + (1.1L_1 - L_2) - \sqrt{X^2 + 0.7^2} \leq 0$

g6: $0.45 - R \leq 0$

g7 (a): $-X \leq 0$

g8 (a): $X + R\cos\frac{\pi}{3} - (L_1 + L_2) \leq 0$

g7 (b): $X \leq 0$

g8 (b): $-X - R\cos\frac{2\pi}{3} - (L_1 + L_2)\cos\frac{\pi}{3} \leq 0$

2.4 Monotoncity Analysis

An attempt was made to solve the problem by monotonicity principles but the problem was too complex to be solved by monotonicity. As seen from the mathematical model the monotonicity of the variables in the objective function was not known as the variables were included in the nonlinear terms of the function. Also the monotonicities of the variables (θ_1 and θ_2) were not apparent.

2.5 Optimization Study

The optimization model analyzes human motion. The fmincon function in Matlab was used to implement the Interior-Point Algorithm used to determine the optimal solution. The flow chart for the computer algorithm is shown below (Figure 7).

The fmincon function starts with initial points of R (crank length) and X (horizontal position) together with set of constraints which investigate the case when X is positive. The objective is a function of R and X. Since the objective function is an integral over different values of crank angle (Θ_3) the stroke length of $\pi/3$ is divided into 6 equal intervals. For each interval (i.e. value of Θ_3 corresponding values of Θ_1 and Θ_2 are found using the two equality constraints h_1 and h_2. This is done by using the fsolve command in Matlab. The corresponding seven values of Torque are calculated. The summation gives the integral over the total stroke length of $\pi/3$. This value is maximized iteratively by the fmincon command till a maximum is found. The procedure is repeated for the second case when X is negative. The maximum values of both the cases are compared to find the maximum and then the corresponding values of R and X are stored.

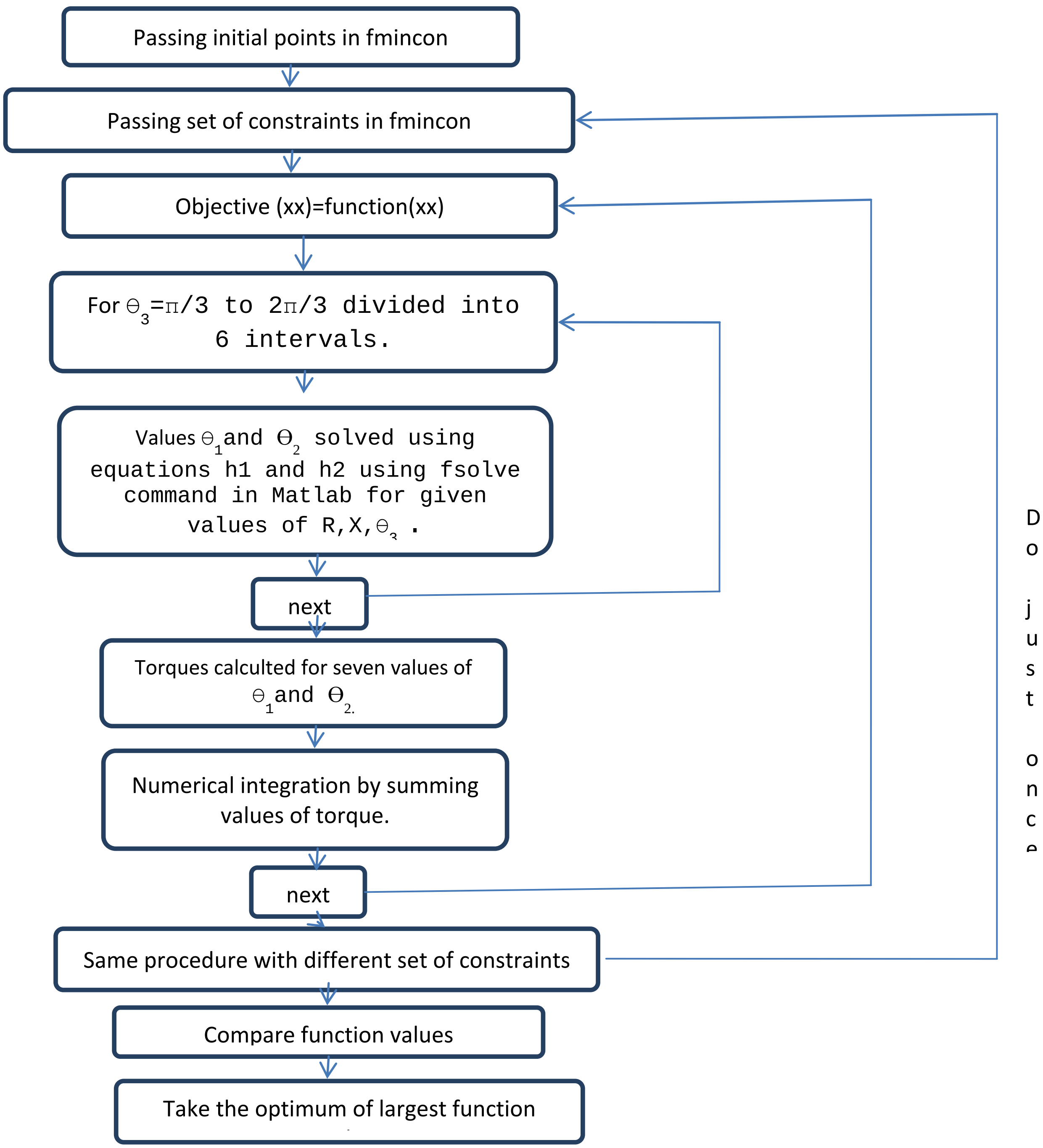

Figure 7: Flow chart for algorithm used in optimization.

Results

The algorithm used was Medium scale SQP, Quasi Newton with Line Search.

The results are tabulated below.

SL no	Starting Points		Final Points			
	R(m)	X(m)	Ropt(m)	Xopt(m)	Ropt(cm)	Xopt(cm)
1	0	0	0.574476	-0.01776	57.4476	-1.7762
2	0.5	0.5	0.5743	0	57.43	0
3	0.75	-0.5	0.57214	-0.01892	57.21398	-1.89224
4	1	-1	0.574273	-1.36E-20	57.42727	-1.4E-18
5	2	1	0.574477	-0.01776	57.44775	-1.77613
6	5	0	0.5743	0	57.43	0
7	10	10	0.574273	0	57.42727	0
8	100	100	0.572113	-0.01894	57.21126	-1.89438
9	100	-200	0.574273	0	57.42727	0
10	0	-10	0.573103	-0.01845	57.31034	-1.84481

The table shows the value of the final points obtained by entering different starting points. From the table we can see that the optimum found is local and not global. The active constraints are g5 and g8. From the table we can deduce that the probable optimum values of R are 0.5743 m and value of X is 0 m. These distances are measured from the shoulder joint. The KKT norm at this point is 1.65E-07(~0) and constraint violation is 7.4e-10(~0). Thus this point is a KKT point and could be an optimizer.

Runs with the variables R and X scaled by a factor of 1000 were also carried out but yet a global optimum was not found. However, again the values of R as 574.3 mm and X as 0 mm had a KKT norm close to zero. [Appendix B-II]

Interpretations of Results

Although we have not been able to find a global solution, the results obtained are more than satisfactory when we consider practical implications. From the table we can easily make out that the optimum value of R lies between (0.570-0.575) m or (57 to 57.5) cm and value of X is (0-1.8) cm. R is the crank length and X is the distance measured from the shoulder joint. A tolerance of 0.5 cm for the crank length and 2 cm for the position of the wheel center is sufficient. This is because while modeling we have made assumptions about the point of application of force at the centre of the palm. This will change from user to user and changes with time for a particular user. The crank lever is attached to the shaft which has a diameter hence the effective lever length can vary by 1 cm. The position of shoulder joint varies (by 2 cm) with physical attributes of the user, bone thickness, etc. Thus a tolerance of 2 cm is sufficient for X (the horizontal position of crank with respect to the shoulder). Thus we can say that for the 95% male the values of R (Crank length) and X (position of lever with respect to the shoulder) should be 0.57m and 0m.

Parametric Study

The following table gives the upper body configuration of males and females.

Limb	Male White			Female White		
	5th	50th	95th	5th	50th	95th
Upper arm link	28.6	30.4	32.3	26.1	27.8	29.5
Forearm link (ulna)	25.6	27.1	28.7	22.7	24.1	25.5
Forearm link (Radius)	25.9	27.5	29.2	22.7	24.1	25.5
Thigh link	40.4	43.2	46.1	36.9	39.5	42.1
Shank link	38.9	42.1	45.3	34.7	37.4	40.0

Figure 8: Link Length values in cm. (Webb ASSOC, 1978)

It was decided that the wheelchair was to be designed for a 95% male. Thus the values of L_1 and L_2 from the table L_1 = 32.3 cm or 0.323 m; L_2 = 28.7 cm or 0.287 m.

95% of people	Length of shoulder L_1(m)	Length of elbow L_2(m)	Mass of shoulder M_1(kg)	Mass of elbow M_2(kg)	α_1	α_2
Males	0.323	0.287	2.7524	2.18226	0.3017	0.1924
Females	0.295	0.255	2.2525	1.73893	0.1488	0.1011

The configuration is studied for a 95% female and the results are reported for a 95% female. The results obtained again vary with starting points indicating that they are local and not global. However by examining the results we can say that the optimum values of crank length **R is 57.32 cm** and value of X(horizontal distance from shoulder) is **0 cm** [Appendix B-III].

2.6 Conclusion

The results indicate that the length of the crank and its position is not much affected by the occupant being male or female (both 95%).The maximum torque that a female can apply is around 70% the maximum a male can apply. In both the cases the lever length is 57 cm and it is attached to the wheel center which is almost collinear to the shoulder joint of the occupant (X~0). The result of X (~0) is very much expected. The body undergoes extension in the wheeling technique which is similar to the body configuration for the new lever mechanism. The wheelchairs available today do have the shoulder joint and centre of the wheel in the same line. Thus we could expect a similar result in the new drive mechanism.

As a wheelchair drive mechanism is very much affected by the physical attributes of the occupant it is often difficult to find a single optimum location of controls. Fitting individuals to the wheelchair is a customizing task. This project aims at customizing the wheelchair setup with respect to an individual’s physical attributes. For practical purposes a therapist (on basis of physical attributes i.e. height and body weight) using a similar algorithm can recommend a wheelchair to a patient.

3. Gears – Karthik Reddy Kothakota

3.1 Problem Statement

The objective of this subsystem is to study and analyze the dimensions of a set of gears and the fatigue life of the gears. This subsystem analysis deals with finding the optimum value of the dimensions of the gear such that fatigue strength of the gear set is maximum (i.e. C^2_{Li} is lowest), represented by the factor, C^2_{Li}. The material being considered for the gear and the pinion is machined high carbon steel.

3.2 Nomenclature

Symbol	Name	Units/Value
P_d	Diametric Pitch	mm
d	Pitch Circle Diameter	mm
b	Face Width	mm
Subscript g	Gear	-
Subscript p	Pinion	-
F_t	Force Transmitted	350 Newton (N)
K_v	Velocity Factor	2.0 (no unit)
K_o	Empirical factor of loading	1.0 (no unit)
K_m	Mounting factor	1.6 (no unit)
S_n'	RR Moore endurance limit	517 N/mm^2
C_s	Surface factor	0.7 (no unit)
K_r	Reliability factor	0.8 (no unit)
K_{ms}	Mean stress factor	1.4 (no unit)
J	Geometry factor	0.35 (no unit)
C_p	Elastic coefficient	206.8 kN/mm^2
I	Geometry factor	
S_H	Effective surface fatigue strength	N/mm^2
S_{fe}	Reference value of surface fatigue strength	448 N/mm^2
C_{Li}	Surface fatigue life factor	
C_R	Reliability adjustment factor	1
N	Number of teeth	
T	Torque to be	262.5 x10^6 N-mm

	transmitted	
ϕ	Pressure Angle	20^o
S_n	Effective endurance	N/mm^2
GR	Gear Ratio	

3.3 Mathematical Model

3.3.1: Objective Function

Objective function:

$$\min C_{Li}^2 = \frac{K_s}{b}\left(\frac{1}{d_p^2} + \frac{1}{d_g d_p}\right)$$

$$K_s = \frac{4C_p^2 K_v K_o K_m T}{\cos\phi \sin\phi \, S_{fe}^2 C_R^2} = 3 \times 10^{12}$$

3.3.2: Constraints

Bending Stresses

The first constraint on the gear tooth is that it should be able to resist bending stress that occurs when the force to be transmitted is applied to the tip of the tooth for which the tooth can act like a cantilever beam. The bending stress equation is given by:

$$\sigma_b = \left(\frac{F_t P_d}{bJ}\right) K_v K_o K_m$$

$$K_b = 1.5 \times 10^5 Nmm$$

This bending stress experienced by the tooth root should be less than the effective endurance limit S_n given by:

$$S_n = S_n' K_r K_{ms}$$

The final constraint for tooth bending stress is:

$$\left(\frac{F_t P_d}{bJ}\right) K_v K_o K_m \le S_n' K_r K_{ms}$$

$$T = F_t\left(\frac{d}{2}\right)$$

The above formula can be simplified by considering a constant K_b and re-arranging the terms in the equation. The gear ratio GR can also be used.

$$K_b = \frac{2TK_vK_oK_m}{K_rK_{ms}}$$

For the gear and pinion material considered is machined medium carbon steel, the value of $K_b = 1.5 \times 10^5 Nmm$.

For the gear and the pinion for a GR of 3, the constraints become:

$$K_bP_d - 106d_gb \leq 0$$

$$GR * K_bP_d - 106d_gb \leq 0$$

Number of Teeth

Minimum number or teeth on the pinion is taken to be 16 teeth, otherwise undercutting of the gear is likely to take place. This applies to the gear also.

$$N_p \geq 16$$

We know that we can reduce this formula for N_p in terms of P_d and d for the gear and the pinion respectively. So for the gear and the pinion, these formulae reduce to:

$$P_d = \frac{N}{d}$$

$$N_g = P_dd_g$$

$$N_p = P_dd_p$$

So the constraints become:

$$16 - P_dd_g \leq 0$$

$$16 - P_dd_p \leq 0$$

Face Width

The face width of the gear set has to lie between given constraints expressed as a function of the diametric pitch.

$$\frac{9}{P_d} \leq b \leq \frac{14}{P_d}$$

So the constraints that come of this system are:

$$9 - bP_d \leq 0$$

$$bP_d - 14 \leq 0$$

Pitch Circle Diameter

The sum of the pitch circle diameters of the gear and pinion should not exceed the distance between the center of the wheel and the base of the chair. Here this distance is taken to be 300mm.

$$d_g + d_p - 300 \leq 0$$

Gear Thickness

The thickness of the gear should not be more than 40mm as the shafts on which both the gears are set have to also accommodate the bearings. This value for the amount of space available for the face width of the gears is given as 40 mm.

$$b - 40 \leq 0$$

Diameter

There is also a basic constraint that the diameter of the gear should be more than that of the pinion. Relating this to the gear ratio gives the mechanical advantage to the system, which is chosen to be 2.

$$GR = \frac{d_g}{d_p} = 2$$

$$2d_p - d_g \leq 0$$

Interfacing

Another important geometric constraint is to prevent interference in the gear tooth i.e. the point of tangency between the pinion and the gear remains on the involute portion of the profile, outside the base circle. This constraint is given by:

$$P_d d_g - 0.085 P_d^2 d_p \left(2d_g + d_p\right) + 1 \leq 0$$

3.3.3 Design Variables

The design variables in this subsystem are the pitch circle diameters of the gear and the pinion d_g, d_p respectively, the diametric pitch P_d and the face width of the mating gears b.

3.3.4 System Parameters

Torque to be transmitted remains constant: T= 262.5 x 10^3 N-mm.

The constants K_s and K_b as given in the equations are evaluated for machined high carbon steel. The required values for these calculations are given below.

K_v	Velocity Factor	2.0
K_o	Empirical factor of	1.0

	loading	
K_m	Mounting factor	1.6
S_n'	RR Moore endurance limit	517 N/mm^2
C_s	Surface factor	0.7
K_r	Reliability factor	0.8
K_{ms}	Mean stress factor	1.4
J	Geometry factor	0.35
C_p	Elastic coefficient	206.8 kN/mm^2
I	Geometry factor	
S_H	Effective surface fatigue strength	N/mm^2
S_{fe}	Reference value of surface fatigue strength	448 N/mm^2
C_{Li}	Surface fatigue life factor	
C_R	Reliability adjustment factor	1
N	Number of teeth	
T	Torque to be transmitted	262.5 x10^6 N-mm
ϕ	Pressure Angle	20 ^{o}
S_n	Effective endurance	N/mm^2
GR	Gear Ratio	2

3.3.5 Summary

Objective function:

$$\min C_{Li}^2 = \frac{K_s}{b}\left(\frac{1}{d_p^2} + \frac{1}{d_g d_p}\right)$$

$$K_s = \frac{4C_p^2 K_v K_o K_m T}{\cos\phi \sin\phi \, S_{fe}^2 C_R^2} = 3 \times 10^{12}$$

Subject to constraints:

g1: $K_b P_d - 125 d_g b \leq 0$

g2: $GR * K_b P_d - 134 d_g b \leq 0$

g3: $16 - P_d d_g \leq 0$

g4: $16 - P_d d_p \leq 0$

g5: $9 - bP_d \leq 0$

g6: $bP_d - 14 \leq 0$

g7: $b - 40 \leq 0$

g8: $2d_p - d_g \leq 0$

g9: $P_d d_g - 0.085P_d^2 d_p\left(2d_g + d_p\right) + 1 \leq 0$

g10: $d_g + d_p - 300 \leq 0$

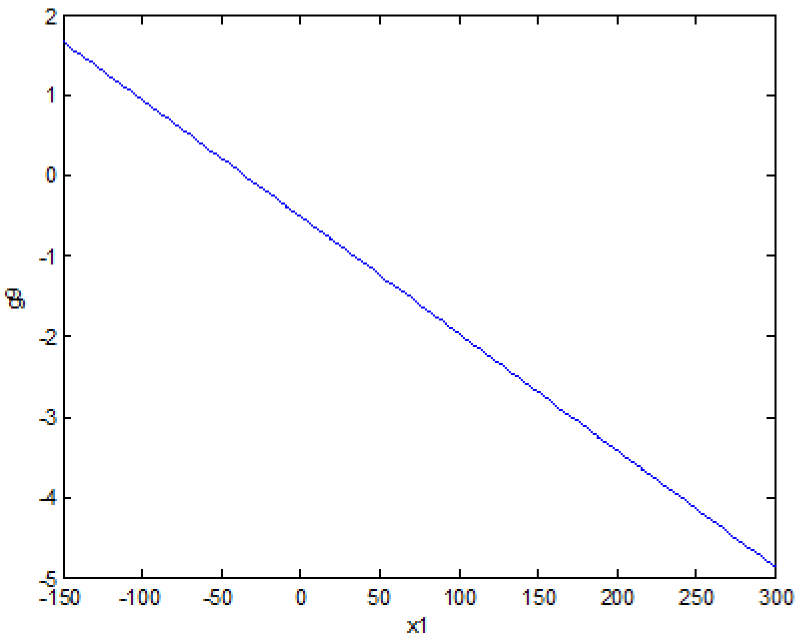

Figure 9: Verification of constraint g9 wrt x1 (x1=-150 to x1=300) and x2=150, x3=70

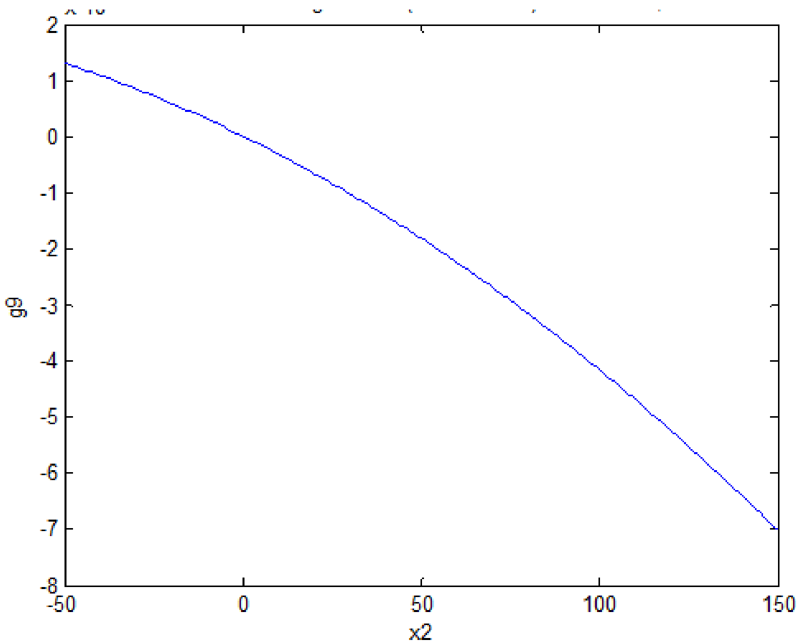

Figure 10: Variation of constraint g9 with x2 (x2 =-50:150) and x1=150, x3=35

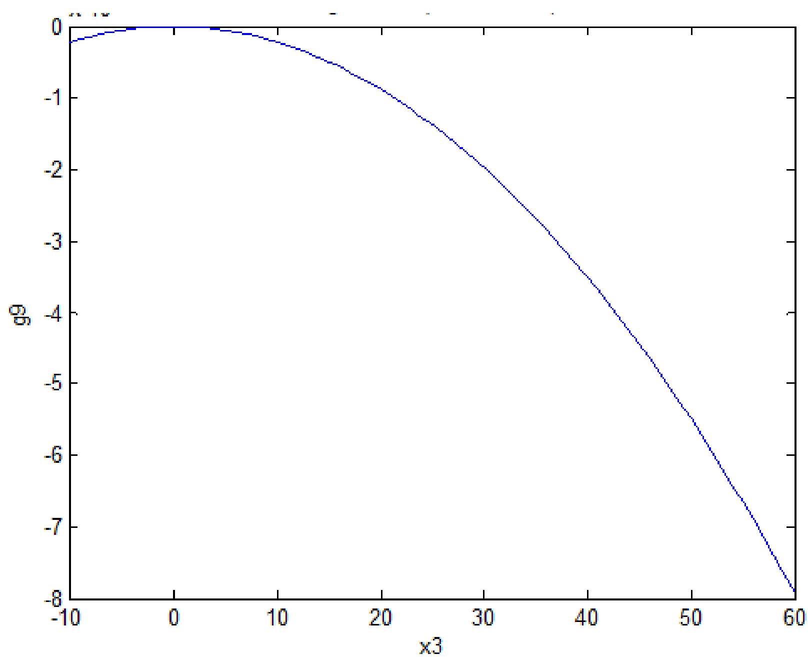

Figure 11: Variation of constraint g9 wrt x3 (x3=-10 to 60) and x1=150, x2=70

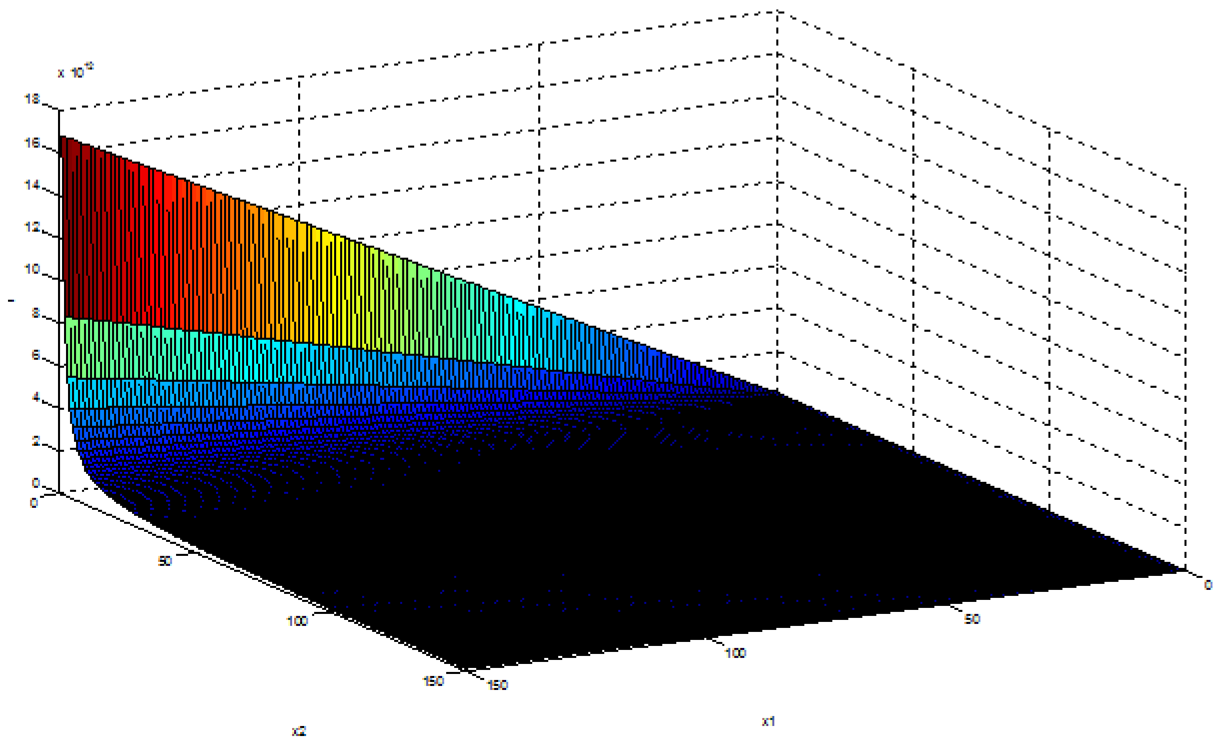

Figure 12: The function surface plot in the domain x1, x2=0 to 150

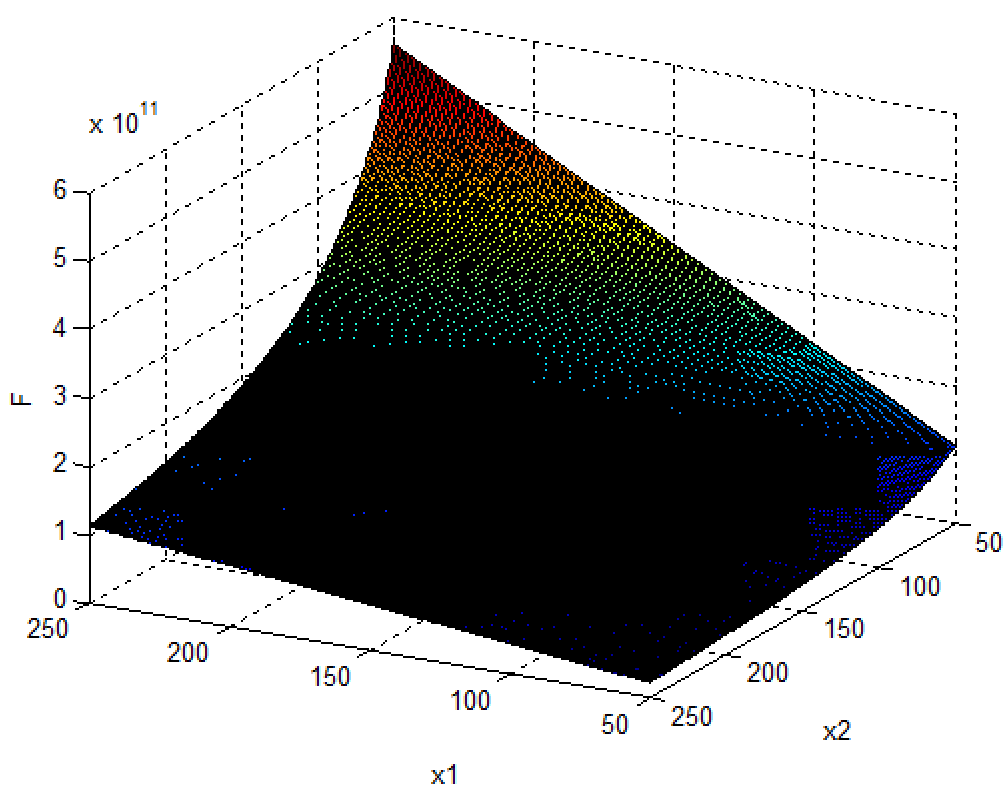

Figure 13: Function variation in the interval of x1, x2=50 to 250

For this design problem, I have chosen the design space to start from 50 for x1 and x2 because if the sudden drop in the function as shown in the surface plots above.

3.4 Monotonicity Analysis

	X_1 (d_g)	X_2(d_p)	X_3(P_d)	X_4(b)
F	-	-		-
G1	-		+	-
G2	-		+	-
G3		-	-	
G4	-		-	
G5			-	-
G6			+	+
G7				+
G8	-	+		
G9	-	-	-	
G10	+	+	+	

x_1,x_2,x_3,x_4 are ≥ 0.

X1: X1 is increasing in g10 and g11. One of these should be active because x1 is decreasing in the objective function. X1 is decreasing in g1, g2, g4, g8 and g9

X2: X2 is increasing in g8 and g10. One of these should be active because x2 is decreasing in the objective function. X2 is decreasing in g3 and g9

X3: X3 is increasing in g1, g2 ang g6. X3 is decreasing in g3, g4 and g9.

X4: X4 is increasing in g6 and g7. One of these should be active because x4 is decreasing in the objectibe function. X4 is decreasing in g1, g2 and g5.

3.5: Optimization and Parametric Study

Using MATLAB the feasible starting points were found. This was done by using the trial and error method where various values of x1, x2, x3, and x4 were substituted in the constraints to see which set of values satisfied the inequalities. The set of values used for the runs are,

	X1	X2	X3	X4
Set 1	160	70	0.4	35

Set 2	170	50	0.45	25
Set 3	190	60	0.4	30

For a gear ratio (GR) of 2

	X_1 (d_g)	X_2(d_p)	X_3(P_d)	X_4(b)	Fatigue Life Factor(x10^8)
Run 1					
Start Values	190	60	0.4	30	
End Value	200	100	0.333	40	0.3375
Run 2					
Start Value	160	70	0.4	35	
End Value	200	100	0.3429	40	0.3375
Run 3					
Start Value	170	50	0.45	25	
End Value	200	100	0.2900	40	0.3375

The constraints g7, g8 and g10 are shown to be active as proven from the Monotonicity Analysis.

For a Gear Ratio of GR=3.

	X_1 (d_g)	X_2(d_p)	X_3(P_d)	X_4(b)	Fatigue Life Factor(x10^8)
Run 1					
Start Values	160	70	0.4	35	
End Value	225	75	0.3357	40	0.533
Run 2					
Start Value	170	50	0.45	25	
End Value	225	75	0.2900	40	0.533

Run 3					
Start Value	190	60	0.4	30	
End Value	225	75	0.33	40	0.533

The obtained seems to be a global minimum because there is no change in the optimum point when the start value was changed. Here also, g7, g8, g10 were active as expected.

Now, the constraint on the sum of the pitch circle diameters was changed from 300 to 250. For GR=2

	X_1 (d_g)	X_2(d_p)	X_3(P_d)	X_4(b)	Fatigue Life Factor(x10^8)
Run 1					
Start Values	160	70	0.4	35	
End Value	166.66	83.33	0.3429	40	0.486
Run 2					
Start Value	170	50	0.45	25	
End Value	166.66	83.33	0.2900	40	0.486
Run 3					
Start Value	190	60	0.4	30	
End Value	166.66	83.33	0.333	40	0.486

This optimum seems to be global as the values did not change for any start value of the problem. Here too, the expected constraint activity is achieved.

Now, the constraint on the sum of the pitch circle diameters was changed from 300 to 250. For GR=3

	X_1 (d_g)	X_2(d_p)	X_3(P_d)	X_4(b)	Fatigue Life Factor(x10^8)
Run 1					
Start Values	160	70	0.4	35	
End Value	187.5	62.5	0.3429	40	0.768
Run 2					
Start Value	170	50	0.45	25	
End Value	187.5	62.5	0.2900	40	0.768

Run 3					
Start Value	190	60	0.4	30	
End Value	187.5	62.5	0.3333	40	0.768

Output Parameters

- Exit Flag Value =1.
- All constraints satisfied.
- First order optimality = 2.91e-10.
- Step Size at exit = 3.33e-12
- Constraint Tolerance = 1e-006
- Function Tolerance = 1e-006
- Constraint Violation = 0

3.6 Interpretation

As the gear ratio increases, the fatigue life tends to decrease (higher value of fatigue life.), for a given distance of the sum of the Pitch Circle Diameters. It needs to be checked whether the solution obtained is global or not, using algorithms that have a capability to find global optimum points. We see that the optimum solution mimics the physics of a gear and pinion system which is used to attain mechanical advantage in the wheelchair.

NOTE: When I performed the optimization using multiple objects of minimizing volume and reducing C^2_{Li}, the Fatigue life factor function was taken as my main objective function and the volume function was taken as a constraint. It was found that the volume constraint was indeed active all the time and the fatigue life factor that was acquired did not for a pareto set with volume but in fact satisfied it as a linear relation. The graph below shows the attempt to model it as a pareto set.

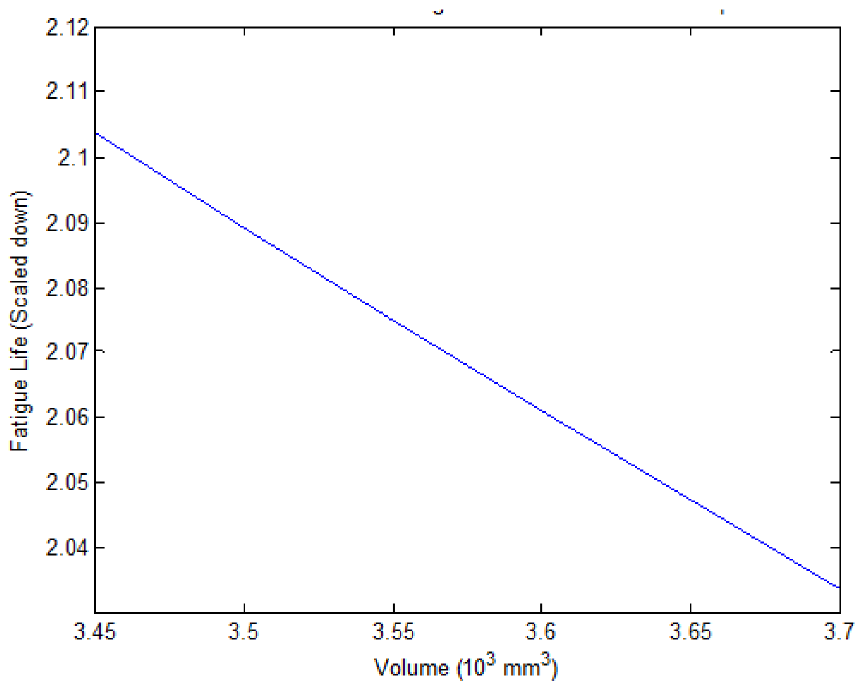

Figure 14: Plot of Volume and Fatigue Life as a linear relationship

4. Shaft – Vishwesh Nampurkar

4.1 Problem Statement

The objective of this project is to minimize the total volume of the shaft. The shaft is supported by two roller bearings. A spur gear and a wheel are mounted on each end of the shaft. The shaft experience torsional and bending loads. This system is to be within certain packaging and weight constraints. The goal of the project is to design a shaft that can transmit the required force, while meeting the packaging constraints.

4.2 Nomenclature Table

SYMBOL	QUANTITY	UNITS
E	Modulus of Elasticity(2*10^5)	N/mm2
Frg2	Radial force on gear2	N
Ftg2	Tangential force on gear2	N
Kb	Bending load factor	
Kt	Torsional load factor	
L1	Length of 1^{st} section of the shaft	mm
L2	Length of 2^{nd} section of the shaft	mm
L3	Length of 3^{rd} section of the shaft	mm
Mt	Twisting Moment	Nmm

Mb	Maximum Bending Moment	N/mm2
R_{AV}	Vertical Reaction at point A	N
R_{BV}	Vertical Reaction at point B	N
R_{AH}	Horizontal Reaction at point A	N
R_{BH}	Horizontal Reaction at point B	N
Te	Equivalent torque acting on shaft	Nmm
V	Total volume of the shaft	mm^3
W	Total weight of the system	Kg
b	Width of the gear	mm
d1	Diameter of 1st section of the shaft	mm
d2	Diameter of 2nd section of the shaft	mm
d3	Diameter of 3rd section of the shaft	mm
dg	Diameter of gear	mm
d_{hub}	Diameter of hub	mm
h	Thickness of the wheel	mm
tb3	Thickness of bearing 3	mm
tb4	Thickness of bearing 4	mm
y	Deflection	mm
τall	Permissible shear stress	N/mm2
ϕ	Pressure angle	
μ	Coefficient of friction between road and wheel	

4.3 Mathematical Model

4.3.1 Objective Function

Minimize the volume of the shaft. It is desired to have as low volume of the shaft as possible.

The volume of the wheel chair should be minimized in order to reduce the overall weight, as well as the overall dimensions of the system.

$$\min \quad V = \frac{\pi}{4}(L1 * d1^2 + L2 * d2^2 + L3 * d3^2)$$

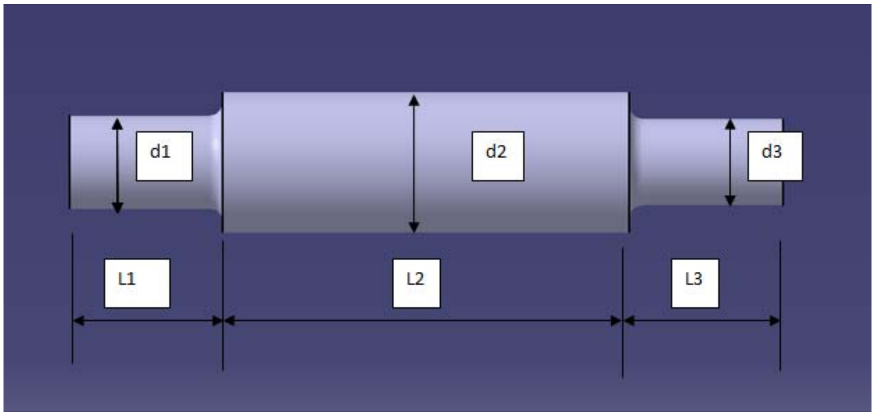

Figure 15: Diagram of Shaft

4.3.2 Constraints

Stress Constraints

The various forces acting on the shaft are the tangential force due to the spur gear acting in the horizontal direction; the radial force due to the spur gear acting in the vertical direction; the total weight of the system acting in the vertical direction; and the horizontal force acting on the shaft due to the wheel acting in the horizontal direction.

For vertical loading the reactions are:

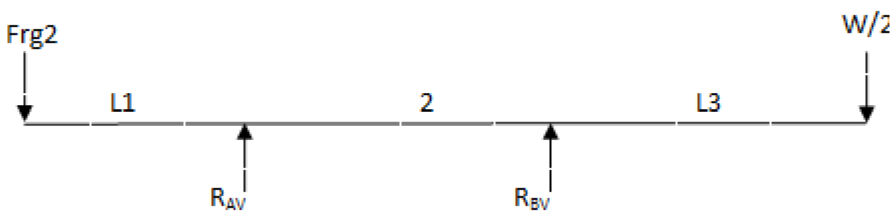

Figure 16: Reactions on the shaft

$$R_{AV} = \frac{Frg2 * (L1 + L2) - \frac{W}{2} * L3}{L2} = \frac{1820(L1 + L2) - 715 * L3}{L2}$$

$$R_{BV} = \frac{\frac{W}{2} * (L2 + L3) - Frg2 * L1}{L2} = \frac{715(L2 + L3) - 1820 * L1}{L2}$$

The vertical bending moments at points A and B are:

$$M_{AV} = Frg2 * L1 = 1820 * L1$$

$$M_{BV} = \frac{W}{2} * L3 = 715 * L3$$

For horizontal loading the reactions are:

$$R_{AH} = \frac{Ftg2 * (L1 + L2) - \mu * \frac{W}{2} * L3}{L2} = \frac{5000(L1 + L2) - 500 * L3}{L2}$$

$$R_{BH} = \frac{\mu * \frac{W}{2} * (L1 + L2) - Ftg2 * L1}{L2} = \frac{500(L2 + L3) - 5000 * L1}{L2}$$

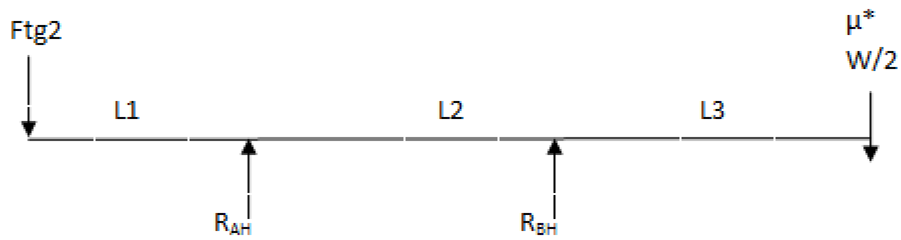

Figure 16: Forces acting on the shaft

The horizontal bending moments at points A and B are:

$$M_{AH} = Ftg2 * L1 = 5000 * L1$$

$$M_{BH} = \mu * \frac{W}{2} * L3 = 500 * L3$$

Bending moments at various points on the shaft will be function of the forces and lengths L1, L2 and L3.

We find out the maximum bending moments at various points on the shaft and select the point which has maximum resultant bending moment.

$$Mb = f(Ftg2, Frg2, R_{BH}, R_{AH}, R_{AV}, R_{BV}, W, L1, L2, L3)$$

Resultant bending moments at A and B are:

$$M_A = 5320 * L1$$

$$M_B = 868 * L3$$

The maximum torque acting on the shaft is known to us:

$$Mt = \mu \frac{W}{2} D = 150000\ N * mm$$

Thus by ASME code we can find out the equivalent torque acting on the shaft.

$$Kb = 2$$

$$Kt = 1.5$$

$$Te = \sqrt{(Kb * MA)2 + (Kt * Mt)2}$$

$$Te = \sqrt{113.2096 * 10^6 * (L1)2 + (5.0625)10}$$

Thus, stress acting on the shaft must be less than permissible shear stress

$$g1: \frac{5.09\sqrt{113.2096 * 10^6 * 2 * L1 + (5.0625) * 10}}{d1^3} - \tau all \leq 0$$

Deflection Constraints

Due to loading of the gears, the shaft is subjected to deflection at the end of the shaft, where gears are attached. The portion of the shaft acts like a cantilever beam and is subjected to a point load due to the radial force of the gear.

We have deflection,

$$y = \frac{\mathrm{Frg2} * \mathrm{L1}^3}{3 * \frac{\pi}{64} * d1^4 * E}$$

$$y = 0.06179 \frac{L1^3}{d1^4}$$

Permissible deflection must be less than the addendum of the gear. It is assumed that permissible deflection is equal to 1 mm.

$$g2: \frac{L1^3}{d1^4} - 16.18 \leq 0$$

Slope Constraints

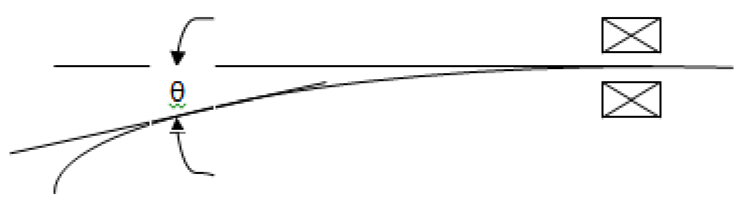

Figure 17: Slope of the beam due to deflection

Due to the deflection of the shaft there will be a slope at the supports. This slope has to be less than 0.003°. If the slope is more than the specified value, then there will be some chipping of the softer material. This will result in the failure of either the shaft or the bearings. In order to avoid the problem we need to restrict this deflection below a certain value.

$$\theta = \frac{\mathrm{Frg2} * \mathrm{L1}^2}{2 * \frac{\pi}{64} * d1^4 * E}$$

$$\theta = 0.09269 \frac{L1^2}{d1^4}$$

The permissible deflection must be less than 0.003° that is $5.2359*10^{-4}$ radians

$$g3\text{: } \frac{L1^2}{d1^4} - 5.648424 * 10^{-3} \leq 0$$

Packaging Constraints

There are some restrictions on the shaft dimensions; this will add some constraints on the system.

The shaft must have a step in order to locate support bearings.

$$d1 < d2$$

$$d3 < d2$$

These are set constraints and can be ignored from the model.

The ratio of the bigger diameter and smaller diameter must be greater than or equal to 1.1. If this ratio is very small it may not restrict the bearing.

$$\frac{d2}{d1} \geq 1.1$$

$$g4\text{: } 1.1d1 - d2 \leq 0$$

$$\frac{d2}{d3} \geq 1.1$$

$$g5\text{: } 1.1d3 - d2 \leq 0$$

We have designed the shaft for the smallest diameter that is d1, thus we must have d3 and d2 greater than d1. Now d2 is always greater than d1 since we have a stepped shaft. Thus d1 must be greater than or equal to d3.

$$d3 \geq d1$$

$$g6\text{: } d1 - d3 \leq 0$$

If the length of the shafts is too long, the width of the wheelchair increases and then it will not pass through the standard doors. Thus, total length of the shaft must not be longer than L.

$$L1 + L2 + L3 \leq 130$$

$$g7: L1 + L2 + L3 - 130 \leq 0$$

The length L1 must be greater than the thickness of the gear as well as the support bearing.

$$25 \leq L1$$

$$g8: 25 - L1 \leq 0$$

The length L3 must be greater than the thickness of the wheel as well as the support bearing.

$$35 \leq L3$$

$$g9: 35 - L3 \leq 0$$

The length L2 in the central portion of the shaft must be greater than, the maximum length of the overhanging part, which is L1 or L3. In this project we have L3 greater than L1.

$$L3 \leq L2$$

$$g10: L3 - L2 \leq 0$$

Manufacturing Constraints

Due to manufacturing constraints the minimum diameter of the shaft, which can be produced, is given as 3 mm.

$$g11: 3 - d1 \leq 0$$

$$g12: 3 - d2 \leq 0$$

$$g13: 3 - d3 \leq 0$$

4.3.3 Design Variables

The design variables are the lengths of each sections of the shaft L1, L2, L3 and also the diameters of the various sections of the shaft d1, d2 and d3.

4.3.4 System Parameters

Permissible shear stress will be design parameter which will be dependent on the material used for the shaft.

$$\tau all = \begin{cases} 0.75 * 0.18 * SUT = 94.5\ /mm2 \\ 0.75 * 0.3 * SYT = 96.75\ N/mm2 \end{cases} \quad \text{whichever is smaller.}$$

The material used is for the shaft is a steel alloy which has ultimate tensile strength (SUT) of 700N/mm^2 and tensile yield strength (SYT) of 430N/mm^2.

τall =94.5 N/mm2

Total weight of the system, W = 1430 N.

Diameter of the wheel, D = 600 mm.

Diameter of the gear, dg = 60 mm.

Ftg2 = 2*Mt/dg = 5000 N

Frg2 = Ftg2 * tan ϕ = 1820 N (with ϕ=20°)

Coefficient of friction, μ= 0.7

Maximum length of the shaft will be the design parameter, so that the wheel chair passes through a standard door. Thus the total length must be less than 130 mm

L=130mm.

Face width of the gear 'b' is a parameter that is a design variable for the gear sub system, and also the track width 'h' is a design variable for the wheel sub system.

Assuming b= 10 mm,

Width of bearings, tb3 = 10 mm and tb4 =10 mm

Thickness of wheel, h= 20 mm

4.3.5 Summary

$$\min V = \frac{\pi}{4}(L1 * d1^2 + L2 * d2^2 + L3 * d3^2)$$

Subject to:

$$g1:\ \frac{5.09\sqrt{113.2096 * 10^6 * 2 * L1 + (5.0625) * 10}}{d1^3} - \tau all \leq 0$$

$$g2: \frac{L1^3}{d1^4} - 16.18 \leq 0$$

$$g3: \frac{L1^2}{d1^4} - 5.648424 * 10^{-3} \leq 0$$

$$g4: 1.1d1 - d2 \leq 0$$

$$g5: 1.1d3 - d2 \leq 0$$

$$g6: d1 - d3 \leq 0$$

$$g7: L1 + L2 + L3 - 130 \leq 0$$

$$g8: 25 - L1 \leq 0$$

$$g9: 35 - L3 \leq 0$$

$$g10: L3 - L2 \leq 0$$

$$g11: 3 - d1 \leq 0$$

$$g12: 3 - d2 \leq 0$$

$$g13: 3 - d3 \leq 0$$

4.4 Monotonicity Analysis

Before attempting to implement the optimization problem, it is important to evaluate the objective function and constraints to see if any information about the problem can be extracted. A common method used to evaluate models is monotonicity analysis. This analysis can be used to validate that the problem is well bounded with respect to every variable as well as determine possibly active constraints.

In this section, the results of model analysis for the study are given. In the above mathematical model there are 13 inequality constraints.

	L1	L2	L3	d1	d2	d3
F	+	+	+	+	+	+
g1	+			-		
g2	+			-		
g3	+			-		
g4				+	-	
g5					-	+
g6				+		-
g7	+	+	+			
g8	-					

g9			-			
g10		-	+			
g11				-		
g12					-	
g13						-

L1, L2, L3, d1, d2 and d3 appear in objective function and are strictly increasing. These variables will be bounded below by at least one active constraint. From the table we can see that all the variables are bounded from above and below. Thus the problem is well bounded.

By applying monotonicity principles,

By MP1 g8 is active, thus L1=25

By MP1 g9 is active, thus L3=35

By MP1 g10 is active, thus L3=L2

By MP1 at least one of g1, g2, g3 and g11 is active with respect to d1.

By MP1 at least one of g4, g5, and g12 is active with respect to d2.

By MP1 at least one of g6 and g13 is active with respect to d3.

4.5 Optimization and Parametric Study

Due to the fact that the resistance objective function was smooth and could be calculated very fast, MATLAB was used as the optimization tool. The fmincon function was used to implement the gradient based method used to determine the optimal solution. Three MATLAB files were generated: one that calculated the objective function, one that had all the constraints, and a third that ran the optimization. The optimizer was run for different starting points to ensure that the optimum is global optimum.

	Trial 1		TRIAL 2		TRIAL 3	
	Initial Value	Final Value	Initial Value	Final Value	Initial Value	Final Value
L1(mm)	1	25.0000	29	25.0000	1000	25.0000
L2(mm)	1	35.0000	50	35.0000	1000	35.0000
L3(mm)	1	35.0000	66	35.0000	1000	35.0000
d1(mm)	1	24.2885	107.5	24.2885	1000	24.2885

d2(mm)	1	26.7173	0	26.7173	1000	26.7173
d3(mm)	1	24.2885	0	24.2885	1000	24.2885
Volume(mm^3)	3	6.0379e+004	288.9e+003	6.0379e+004	3e+009	6.0379e+004
No of Iterations	8		14		34	

It is seen that for different values of starting points we get the same volume as the output. Thus, there is global convergence. And the optimum is global.

Constraint Activity:

At the optimum values of the lengths and the diameters, values of each constraint were noted. If any particular constraint is active then, it is satisfied by a pure equality.

$$g1\text{: } \frac{5.09\sqrt{113.2096 * 10^6 * 2 * L1 + (5.0625) * 10}}{d1^3} - \tau all \leq 0$$

$$g2\text{:} \frac{L1^3}{d1^4} - 16.18 \leq 0$$

$$g3\text{: } \frac{L1^2}{d1^4} - 5.648424 * 10^{-3} \leq 0$$

$g4\text{: } 1.1d1 - d2 \leq 0$

$g5\text{: } 1.1d3 - d2 \leq 0$

$g6\text{: } d1 - d3 \leq 0$

$g7\text{: } L1 + L2 + L3 - 130 \leq 0$

$g8\text{: } 25 - L1 \leq 0$

$g9\text{: } 35 - L3 \leq 0$

$g10\text{: } L3 - L2 \leq 0$

$g11\text{: } 3 - d1 \leq 0$

$g12\text{: } 3 - d2 \leq 0$

$g13\text{: } 3 - d3 \leq 0$

Thus, g*= [g1, g2, g3, g4, g5, g6, g7, g8, g9, g10, g11, g12, g13,]

= [0 -16.1413 -0.0037 0 0 0 -35 0 0 0 - 22. 2111 -24.7322 - 22. 2111]

From the above values we conclude that's g1 g4 g5 g6 g8 g9 and g10 are active.

The figure below shows the convergence of the solution for the first trial.

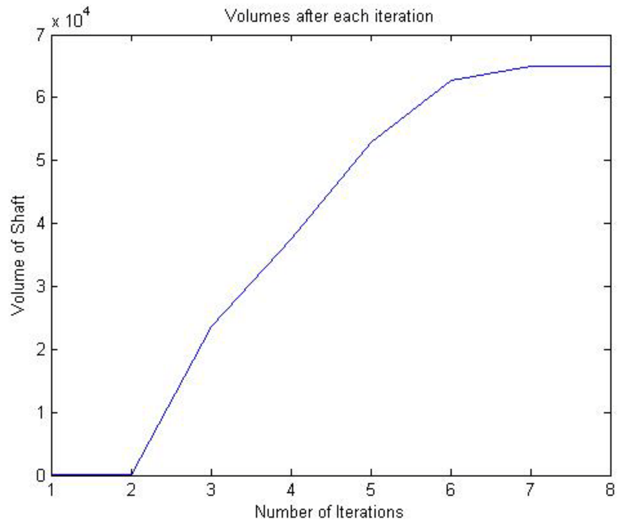

Figure 18: Plot showing the volume of the shaft for various iterations.

At the starting point the volume is 3 mm^3. With more number of iterations we see that the volume keeps on increasing. The rate at which the volume increases is high for initial number of iterations, indicating a large slope. But after 6^{th} iteration the volume increases slightly with a small slope. The optimum is achieved at the 8^{th} iteration, thus the optimum volume is 6.5054e+004 mm^3.

A parametric study of the system was performed to explore the effects of changes in each parameter on the optimum while keeping the other parameters constant, and also the effects of changes in a combination of all the parameters on the optimum. The parametric tables are presented along with the curves indicating the variations of the optimum as functions of parameter changes within a certain range.

a) Material of the shaft:

   Desirable for shaft materials are:

   1) Sufficient high strength.
   2) A low sensitivity to stress concentration.
   3) Ability to withstand high temperatures.
   4) High wear resistance.
   5) Good machining ability.

To meet the requirements shafts are mostly made from plain carbon steels ranging from C25 to C50. Shafts are made from alloy steels of various grades to minimize the diameter and increase the wear resistance. Thus a parametric study was performed to observe the change in the volume of the shaft with respect to the materials used. Table shows the result of parametric study.

No.	MATERIAL	STRENGTH(N/mm2)	d1(mm)	VOLUME(mm3)
1	C20	440	28.3541	8.2285e+004
2	C50	660	24.7696	6.2795e+004
3	40 Cr 1 Mo	720	24.2885	6.0379e+004
4	35Mn 2 Mo	760	24.0615	5.9256e+004
5	40 Cr 3 Mo 55	1350	19.5129	3.8970e+004

Graphs below show the trend of changes in volume and d1 with respect to different materials selected. It is seen that there is a drastic reduction in volume when the material is changed from C20 to C 50. There is not much difference in volumes between C50 and 35 Mn 2 Mo steel. But if we use 40 Cr 3 Mo 55 the volume again reduces significantly. But this metal alloy is very expensive which will include additional cost constraint in the model. Thus we can conclude that we can select any material from C50 to 35 Mn 2 Mo having ultimate tensile strengths ranging from 660 to 760 N/mm2.

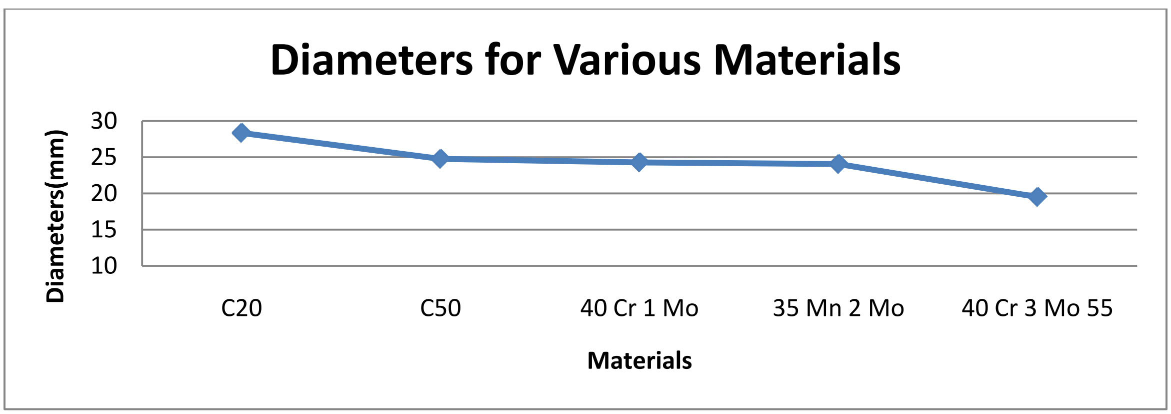

Figure 19: Plot showing the optimized diameter of shaft for various materials.

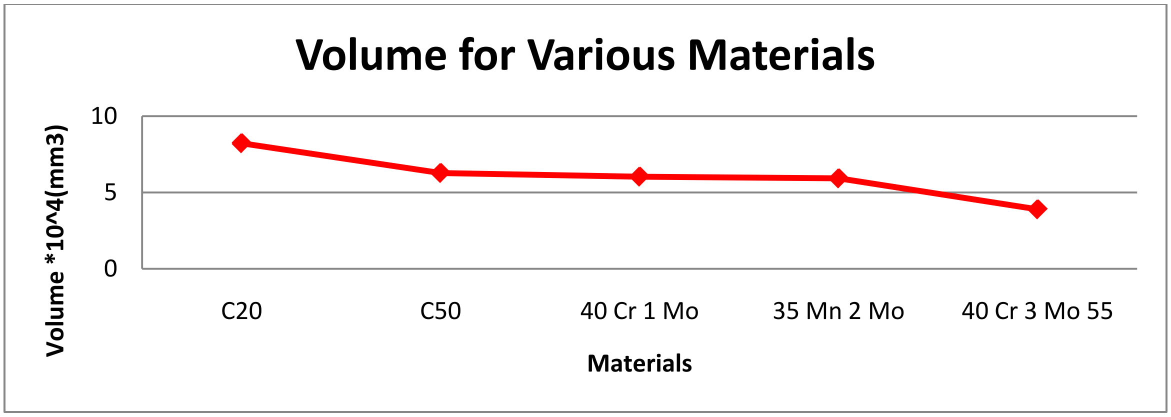

Figure 20: Plot showing the optimized volume of shaft for various materials.

5 The Wheel – Clare McNamara

5.1 Problem Statement

The objective for the wheel subsection is to minimize the mass of the wheel. The wheel needs to have minimum mass in order to reduce the amount of force needed to drive the wheelchair. The tradeoffs for this subsystem will be between the wheel and the shaft, the primary subsystem with which the wheel interacts. In minimizing the mass of the wheel, the wheel will want to become as small as possible, however, the hub of the wheel needs to be able to fit around the shaft. Additionally, the wheel needs to provide mechanical advantage, which is a relationship between the radius of the wheel and the radius of the axel. There will also be ergonomic constraints that require the diameter of the wheel to fall into a certain range such that the passenger's interaction with the lever shaft will be comfortable.

A commonly used wheel in manual wheel chair design is a bicycle style radial spoke wheel (7). This wheel consists of an aluminum alloy rim, stainless steel spokes, and an aluminum hub where it connects to the shaft of the gear system. The initial wheel chosen to have 24 spokes; it will be possible to do a parameter study on the number of spokes later in the project. For simplicity in this model, the hub will be taken to be of uniform, solid aluminum cross section, and a tire will be neglected.

Figure 21: Radial spoke wheelchair wheel

Much work has been done on modeling the spoke stresses in a pre-strained spoked wheel such as the one commonly used in wheelchairs. Finite Element Analysis completed by Andrew D. Hartz at Rose-Hulman Institute of Technology was used as reference for describing the stresses in the spokes, as well as the book 'Bicycle Wheel' 3rd Edition by Jobst Brandt. Work on modeling the deflection of a rolling wheel was done by J.P. Hambleton and A. Drescher, of the civil engineering department at the University of Minnesota.

5.2 Nomenclature

Symbol	Quantity	Units
α	angle between the normal to horizontal ground and obstacle	degrees
E_s	Young's Modulus for steel	Pa
g	Gravitational acceleration	mm/s^2
FS	factor of safety	
F_c	critical force	N
F_{tot}	total force acting on the wheel	N
I	moment of inertia	mm^4
m_p	mass of the passenger	kg

m_w	mass of the wheel	kg
m_{wc}	mass of the wheelchair without the wheels	kg
q	average stress over projected length of contact between the wheel rim and obstacle	N/mm^2
$\sigma_{a,y}$	yield stress of aluminum	N/mm^2
r_h	radius of the wheel hub	mm
r_i	inner radius of the wheel rim	mm
r_o	outer radius of the wheel rim	mm
r_s	radius of the spoke	mm
r_{shaft}	radius of the shaft	mm
ρ_a	density of aluminum alloy	kg/mm^3
ρ_s	density of steel	kg/mm^3
t_r	thickness of rim and hub	mm
V_h	volume of the hub	mm^3
V_r	volume of the rim	mm^3
V_s	volume of the spoke	mm^3

5.3 Mathematical Model

5.3.1 Objective Function

The objective function is to minimize the mass of the wheel with respect to its height (radius), thickness, size of the hub, and width of spoke.

Since the density of the material is known, the mass is equal to the volume divided by the density.

$$m = V\rho$$

The volume of the wheel is the combined volume of the rim, the spokes, and the hub.

$$V_r = \pi t_r (r_o^2 - r_i^2)$$

$$V_s = 24\pi(r_i - r_h)r_s^2$$

$$V_h = \pi t_r(r_h - r_{shaft})^2$$

$$V_h = \pi t_r(r_h - 10)^2$$

As seen above, the volume of the hub depends on the radius of the shaft. For this subsystem optimization, this will be taken as a parameter, 10 mm, but when the subsystems are integrated, this will be a linking variable. The rim and the hub are both made from aluminum alloy, and the spokes are made from stainless steel. The total mass is the sum of the volumes of the rim, spokes and hub divided by their respective densities.

The objective function becomes:

$$\min_{r_o, r_i, r_h, r_s t_r} m_w = \rho_a\, \pi t_r(r_o^2 - r_i^2) + \rho_s 24\pi(r_i - r_h){r_s}^2 + \rho_a \pi t_r(r_h - 10)^2$$

5.3.2 Constraints

The wheel, spokes and hub are constrained by a number of factors. There are packaging constraints on the wheel, as it cannot be too tall, or the lever will be in an ergonomically incorrect location. It cannot be too wide, as the wheel chair needs to be able to meet the standards of manual wheel chairs, and fit through standard doorways. Additionally, it cannot be too small, or it will not achieve the mechanical advantage offered by the current manual wheel chair. There are load constraints, as the wheels are the prime carriers of the load of the wheelchair. They must be able to support the load of the wheelchair and its passenger without buckling. Additionally there are strength constraints, because the rim of the wheel must be strong enough to avoid deformation from obstacles it meets on the road.

Packaging Constraints

The outer radius of the wheel is constrained by the maximum height of the armrest of the standard wheelchair for ergonomic reasons. If the wheel is higher than the armrest, it will block the passengers reach to the lever. The outer radius also must be greater than the inner radius and the radius of the hub, which is obvious from geometry.

$$r_o \leq 380m$$

$$r_h < r_i < r_o$$

Because just having an inequality relation for the sizes of the radii will not provide good bounds for these variables, it is necessary to define a step size relation between these components of the model.

$$\frac{r_o}{r_i} \geq 1.1$$

$$\frac{r_i}{r_h} \geq 1.1$$

The radius of the hub must be greater than the size of the shaft which is connected to it, again by a step size. The typical shaft diameter is 20mm, so a shaft radius of 10mm will be set as a parameter for this constraint. However, when the subsystems are integrated into the system, this parameter will instead be the variable from the shaft optimization.

$$\frac{r_h}{10} \geq 1.1$$

The shaft must also be large enough to attach all of the spokes to, meaning that the perimeter of the hub must be larger than the perimeter formed by the 24 spokes attached to it.

$$2\pi r_h \geq 24 * 2r_s$$

The thickness of the wheels is constrained by the overall width of the standard wheelchair (660 mm) and the width of the seat of the standard wheelchair (457 mm). Both wheels and the additional parts of the drive mechanism must fit in the difference of these two widths (203 mm) so that it can meet current design specifications and be able to fit through standard doorways. If we assume that the additional parts of the drive mechanism (the shaft , gears and lever) have a combined thickness equal to the thickness of the wheels, then each wheels thickness must be a quarter of the total allowable thickness. Again, in the combination of the subsystems, this parameter will be adjusted to take in the variable thicknesses of the other subsystems. The thickness of the wheel must also be a positive, non-zero value.

$$4t_r \leq 203\ mm$$

$$t_r > 0$$

When the subsystems come together for overall system optimization, the thickness of the hub will have to be less than or equal to the length of the section of the shaft that fits into it.
The radius of the spokes is similarly constrained by the width of the thickness of the wheel, which is to say the radius of the spoke cannot be more than half the thickness of the wheel. It must also be a positive, non-zero value.

$$r_s > 0$$

$$2r_s \leq t_r$$

The mechanical advantage will also place a constraint on the outer radius of the wheel. In order for this drive mechanism to be desirable, it must produce a mechanical advantage at least as large as the mechanical advantage provided by the standard manual wheelchair.

$$MA = \frac{r_0}{r_{shaft}}$$

$$r_0 \geq r_{shaft}MA$$

Where r_{shaft} is the radius of the typical wheel axle. For now this is chosen to be a parameter, but when the systems integrate, this will be the shaft radius of the shaft subsystem.

$$r_o \geq (10\ mm)(30.48)$$

$$r_o \geq 305\ mm$$

Strength Constraints

There will be strength constraints on both the spokes and the rim of the wheel. The most common type of failure for a wheel is buckling. There for the design must be optimized such that the wheel will be strong enough to prevent buckling. The stress distribution in a spoked wheel is complicated and not intuitive. It is a common misconception that when a wheel has a force exerted upon it by the axel, the spokes on the top and bottom of the wheel compress and the wheel rim elongates horizontally. In this situation, the stresses would be distributed throughout the spokes. However, this is not true (8). Through modeling with FEM analysis, it has been shown that the stress is concentrated on the single spoke in contact with the rim at the point it is touching the ground (9). Because the stress of the spoked wheel is concentrated and isolated to the spoke which is coming from the rim at the point of contact with the ground, the wheel can be modeled as a beam at this point, and critical force at buckling can be found by using the equation for an Euler column.

$$F_c = \frac{\pi^2 EI}{(KL)^2}$$

Where F_c is the critical force, I is the moment of inertia, L is the unsupported length of column and K is the column effective length. K for a column fixed at both ends, as in the spoke, is 0.5. Spokes are typically solid with a circular cross-section, so the moment of inertia is taken for a beam with a circular cross section

$$I = \frac{\pi r^4}{4}$$

$$F_c = \frac{\pi^3 E_s r_s^4}{4(K(r_i - r_h))^2}$$

This force is the critical force for the spokes, which means that the force being supported by the spoke must be less than this. The force being supported by the spoke is equal to the total force of the system divided by 2, because the force is being supported on 2 wheels (the large wheel on each side of the chair). The factor of three is to account for the safety factor in building the wheels.

$$F_{tot} = \frac{3(m_p + m_{wc})g}{4}$$

$$F_{tot} \leq F_c$$

$$\frac{3(m_p + m_{wc} + 2m_w)g}{2} \leq \frac{\pi^3 E_s r_s^4}{4(K(r_i - r_h))^2}$$

$$\frac{3(m_p + m_{wc} + 2m_w)g}{2} \leq \frac{\pi^3 E_s r_s^4}{4(K(r_i - r_h))^2}$$

Another common source of failure for the wheel is plastic deformation of the rim. This occurs most often when the wheel hits some obstacle and the stress at the point of contact exceeds the yield strength of the rim material. The modeling of a rolling wheel in the presence of plastic deformation was done by J.P. Hambleton and A. Drescher, of the civil engineering department at the University of Minnesota. In this work a rigid wheel which is elastic-perfectly plastic was modeled, moving at steady state and meeting an obstacle. It was found that the stress on the rim upon contact with the obstacle is dependent on the normal force, the projected length of contact between the material and the wheel, and the thickness of the wheel rim (10). This relationship can be described by the equation

$$q = \frac{F_{tot} cos\alpha}{2r_o\, t_r \sin\frac{\alpha}{2}}$$

Where q is the average stress over projected length of contact and α is the contact angle. This average stress can be taken as the von Mises yield condition, and needs to be less than the yield strength for the material in order to prevent plastic deformation for the rim.

$$q \leq \sigma_{a,y}$$

$$\frac{F_{tot} cos\alpha}{2r_o\, t_r \sin\frac{\alpha}{2}} \leq \sigma_{a,y}$$

This relation will place a constraint on the thickness of the rim of the wheel. This constraint also introduces the variable α, which is equal to the angle that the obstacle makes with the normal to the horizontal. By geometry, it can be seen that $0 \leq \alpha \leq 90$.   In particular, we want to look at which α will produce the greatest stress on the wheel, which is 45°.

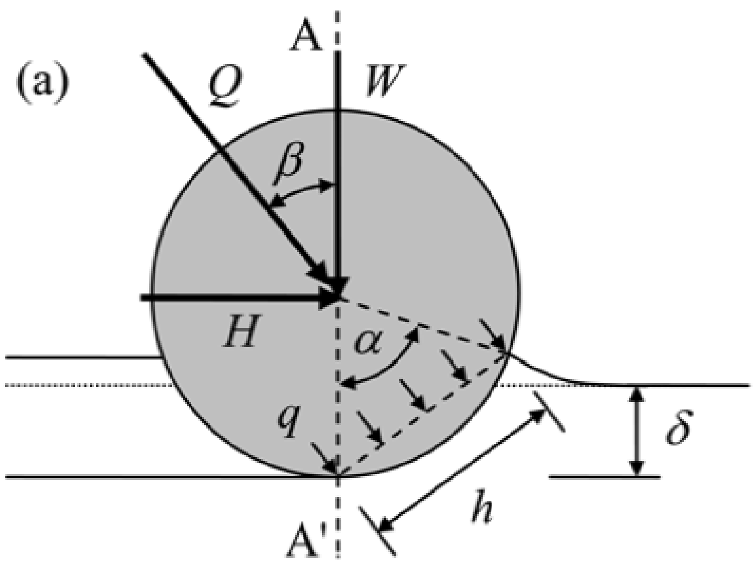

Figure 22: Diagram of stresses on a wheel meeting an obstacle (10).

5.3.3 Design Variables

The variables of the sub system are the inner and outer radius of the rim of the wheel, the width of the wheel, the thickness of the spokes, the radius of the hub and the thickness of the hub.

5.3.4 System Parameters

The parameters for this sub-system include the mass of the passenger, the width of the total wheelchair, the mechanical advantage of a standard manual wheel chair, the material used in the wheel, the style of wheel, the factor of safety, and the torque that the wheel needs to withstand. Setting the material as a parameter also parameterizes the yield strength of the different materials, and the density of the materials.

For the mass of the passenger, a man of the 95th percentile was chosen. The mass is taken to be 116 kg (11).

The width of a standard wheelchair is 660 mm, which includes the rail required to move a manual wheel chair. Since the drive mechanism will not require this rail, using this as a parameter will allow us to make the wheel of our system wider than the standard if necessary, and still meet the government wheel chair standards (6).

The style of wheel is chosen to be a 24 radial spoke wheel.

The standard wheelchair wheel comes in diameters of 22", 24" and 26". For this project the parameter was chosen to be 24" = 609.6mm. The standard axel diameter is 20mm. For a wheel,

$$Mechanical\ Advantage = \frac{r_o}{r_{shaft}}$$

and the standard mechanical advantage = 30.48.

The materials used in the wheel are chosen to be aluminum alloy 6061 for the rim and hub and stainless steel 304 for the spokes. The material properties of aluminum alloy 6061 are (12):

Density	ρ_a	2.7e-6 kg/mm^3
Young's Modulus	E_a	69 GPa
Tensile Strength	$\sigma_{a,t}$	125 MPa
Yield Stress	$\sigma_{a,y}$	55 N/mm^2
Percent elongation		25-30%

The material properties of stainless steel 304 are (13):

Density	ρ_s	8000 kg/m^3
Young's Modulus	E_s	193 GPa
Tensile Strength	$\sigma_{s,t}$	515 MPa
Yield Stress	$\sigma_{s,y}$	205 MPa
Percent elongation		40%

It is necessary in this subsystem to use the total force acting on the wheel as part of some of the constraints. In order to do this it is necessary to parameterize the mass of the passenger in the chair, as well as the mass of the chair without the wheels. Using the upper limits for standard manual wheel chairs, the mass of the wheel chair was selected to be 30 kg (the majority of wheel chairs are less than 20 kg). Also necessary for these constraints is to include a factor of safety. Here it is chosen to be 3.

5.3.5 Summary

The minimization of the mass of the wheel is summarized below along with the constraints that were previously derived.

Objective function

$$\min_{r_o, r_i, r_h, r_s t_r} m_w = \rho_a \pi t_r (r_o^2 - r_i^2) + \rho_s 24\pi (r_i - r_h) r_s{}^2 + \rho_a \pi t_r (r_h - 10)^2$$

Subject to

g1= $r_0 - 380 \le 0$

g2= $1.1 r_h - r_i \le 0$

g3= $1.1 r_i - r_o \le 0$

g4= $11 - r_h \le 0$

g5= $4 t_r - 203 \le 0$

g6= $r_s - \frac{t_r}{2} \le 0$

g7= $305 - r_o \le 0$

g8= $48r_s - 2\pi r_h \leq 0$

g9= $\frac{F_{tot}\cos 45}{2r_o\, t_r \sin 22.5} - \sigma_{a,y} \leq 0$

g10= $F_{tot} - \frac{\pi^3 E_s r_s^4}{4(K(r_i - r_h))^2} \leq 0$

$r_o, r_i, r_h, r_s, t_r, > 0$

where $F_{tot} = \frac{3(m_p + m_{wc} + 2m_w)g}{2}$

Feasible Solution

A feasible model is found in values of a standard bicycle or wheelchair wheel. For example, a 0.6604 m (26in) wheel, which is a common size for wheel chairs, would give the following feasible solution:

r_o =330 mm

r_i= 300 mm

r_h=25 mm

r_s=3 mm

t_r=38 mm

which will give a feasible solution of

m_w =7.842kg

5.4 Monotonicity Analysis

Monotonicity Analysis is applied to the model to check for well-boundedness as well as to check for active constraints and possibly reduce the model.

	t_r	r_o	r_i	r_h	r_s
m_w	+	+	-	+	+
g1		+			
g2			-	+	
g3		-	+		
g4				-	
g5	+				
g6	-				+

g7		-			
g8				-	+
g9	-	-			
g10			+	-	-

The conditionally active set includes g3, g4, g6, g7, g8, g9 and g10. From monotonicity principle 1, it is evident that one constraint is active, g10.

5.5 Optimization and Parametric Study

The wheel model was optimized using Matlab's optimization function fmincon. This program was chosen because the model is entirely algebraic.

The results of fmincon, using the initial point found before, were as follows:

r_o= 305 mm

r_i= 277 mm

r_h= 251 mm

r_s= 0.8 mm

t_r= 1.6 mm

f_{opt}= 1.05 kg

A quick look at a couple feasible starting points found that there was not obvious convergence, so a design of experiments creating a Latin hypercube was done to choose 10 initial points to look at for convergence.

The initial points chosen are:

	r_o	r_i	r_h	r_s	t_r
point 1	58	522	27	5	90
point 2	995	161	96	9	82
point 3	309	375	1	3	55
point 4	405	859	59	4	75

point 5	150	290	79	2	65
point 6	551	786	88	0.8	7
point 7	266	605	13	8	35
point 8	610	904	42	7	15
point 9	763	42	33	6	22
point 10	888	494	65	1	42

Covergence search:

initial point	output r_o (mm)	output r_i (mm)	output r_h (mm)	output r_s (mm)	output t_r (mm)	f_{opt} (kg)
point 1	305	277	114	1.8	3.6	1.1
point 2	305	164	92	1.3	2.7	1.8
point 3	305	277	114	1.8	3.6	1.1
point 4	305	277	53	2.4	4.8	1.6
point 5	305	277	114	1.8	3.6	1.1
point 6	670	1001	164	0	341	-0.0015335
point 7	305	277	114	1.8	3.6	1.1
point 8	305	277	114	1.8	3.6	1.1
point 9	305	39	35	0.3	0.6	0.4
point 10	314	285	259	0.9	1.6	1.1

From the design of Latin hypercube analysis, it is evident that initial points 1, 3, 5, 7, and 8 all converge to the same values, and points 6, 9, and 10 are all infeasible designs. This suggests that the optimum values of this model are as follows:

r_o= 305 mm

r_i= 277 mm

r_h= 114 mm

r_s= 1.8 mm

t_r= 3.6 mm

f_{opt}= 1.1 kg

Parameter Study

Another common material used for building high performance spoked wheels is carbon fiber. Carbon fiber may be used for the entire wheel-spoke-hub system, instead of using an aluminum alloy and a steel alloy. Nylon 6 with carbon fiber composite is chosen for a parameter study on the wheel. It has an average density of 1.27kg/mm^3, an ultimate tensile strength of 167MPa and an average Elastic modulus of 14.5 GPa. Using these material values, the following results were obtained:

r_o= 305 mm

r_i= 277 mm

r_h= 118 mm

r_s= 4.5 mm

t_r= 9.1 mm

f_{opt}= 1.3387 kg

Here, some significant differences and similarities can be seen. The outer radius of the wheel has very minimal changes, which is good, because this is the variable that will change the overall system design most significantly, since it will affect the length of the lever arm. This spoke radius also has gotten bigger to make up for the lower Elastic modulus of the composite. Interestingly, though the density of the carbon fiber composite is less than half that of the aluminum alloy and much lower than the steel, the optimal mass of the wheel ends up roughly the same due to the compensation of the length and radius of the spokes.

5.6 Conclusion

Based on current wheel designs, these numbers seem to make sense with one major discrepancy, the thickness of the wheel rim and hub. The value determined here is much smaller than typical values (19.05mm – 50.8mm). This means there is probably some constraint needed to put a lower bound on the thickness that has not been considered in this model, alternatively it may reflect the fact that the cross-section of the rim, which was just taken to be a rectangle, is too simple of a simplification, a more accurate representation of the rim cross-section would be a "U" shape.

From these results a few interesting things are evident. As stated before in the monotonicity analysis, constraint g10 is an active constraint. This constraint acts on the spoke radius and length. As found in the background research, the spokes are an integral feature of the wheel, with all the stresses of the system acting on them, so it makes sense that this strength constraint on the spokes is active. Additionally, it is evident that constraint g6 and g7 are active constraints. Constraint g6 is the lower bound on the thickness, which as previously mentioned suggests that there is a constraint missing. When the subsystems are brought together, the thickness of the rim will also depend on the length of the shaft attaching to the hub, as they should be equal in this design, this will probably act as a new lower bound for this variable. Constraint g7 puts a lower bound on the outer radius of the wheel by comparing it to the mechanical advantage of the standard wheel. If mechanical advantage can be made up in the gear subsystem, this constraint could be loosened. It should also be remembered that this variable will also impact the length of the lever handle, so it will also probably be affected during the linking of the subsystems. Constraint g9 is an inactive constraint, which suggests that in this model all of the other constraints act to prevent deformation of the wheel when it hits an obstacle. A possible issue with regards to this constraint is that the cross section of the rim is assumed to be uniformly rectangular. If a more precise description of the cross section were used, this constraint might become active.

Overall the model and the optimization seems to be reasonable, because the results seem to mostly agree with current spoked wheel designs.

6. System Integration

We choose to use the objective function from the lever subsystem as the overall objective function for our wheelchair drive mechanism. This choice is made for a few reasons. First of all, the lever is the part of the system that the user of the wheel chair would come into direct contact with, so it is important that optimization that takes into account the user be considered. Additionally, the objective function of the lever, when adjusted for parameters of the other system, interacts directly with both the gears and the wheel, both of which interact with the shaft. Because this objective seemed to capture the most of the total system, we choose to use it for the overall objective.

6.1 Problem Statement

The objective function for the system is to maximize the amount of work done by the lever handle and thus the rest of the system, for a specific passenger body type.

The objective function is thus stated as:

$$\text{Max } W=\int_{\pi/3}^{2\pi/3} T d\theta_3$$

For rotation through an angle of 60^0 or $\pi/3$.

$$T = \alpha_1(227.338 + 0.525\theta_2) + \alpha_2(336.29 + 1.544\theta_2 - 0.0085\theta_2^2 - 0.51\theta_1) - (M_1 + M_2)g \sin\theta_1 \frac{L_1}{L_2} - M_2 g \cos(\frac{\pi}{2} + \theta_1 - \theta_2)\frac{L_2}{2}$$

Where L_1 and L_2 are lengths of the arm sections, and M_1 and M_2 are the masses of the shoulder and the elbow respectively, and α_1 and α_2 are correction factors.

6.2 Subsystem Trade-offs

The subsystems are linked through geometry, because the shaft, wheel and gears physically interact with each other, and thus must agree. Additionally, torque is transmitted from the wheel through the shaft and through the gears.

6.2.1 Lever Handle Constraint Updates

For the lever, the following parameters became variables: (i) r_o, the outer radius of the wheel, (ii) d_g, the diameter of the gear, and (iii) d_p the diameter of the pinion.
In the subsystem optimization r_o was taken to be 0.35m and this included the actual radius of the wheel, the diameter of the gear and the diameter of the pinion.

The constraints that change when this parameter became variables are: $Y = 1.05m - R_{wheel}$

h1: $-L_1 \cos\theta_1 + L_2 \sin\theta_2 + R\cos\theta_3 - 0.7 = 0$

In this constraint, $0.7^2 = Y^2$ where

$$Y = 1.05m - R_{wheel}$$

$$R_{wheel} = r_o + \frac{d_g}{2} + \frac{d_p}{2}$$

After these changes:

h1: $-L_1 \cos\theta_1 + L_2 \sin\theta_2 + R\cos\theta_3 - (1.05 - (r_o + \frac{d_g}{2} + \frac{d_p}{2})) = 0$

Similarly, constraint g5: $1.1R + (1.1L_1 - L_2) - \sqrt{X^2 + 0.7^2} \leq 0$ becomes:

g5: $1.1R + (1.1L_1 - L_2) - \sqrt{X^2 + (1.05 - (r_o + \frac{d_g}{2} + \frac{d_p}{2}))^2} \leq 0$

For constraint g6: $0.45 - R \leq 0$, we adjust the distance of the arm rest from the center of rotation of the lever axis. The height of the armrest from the ground was originally taken to be 0.8 m, but upon further investigation, this is too large of a height, so in the system it is adjusted to 0.68m. The armrest height now becomes $0.68 - (r_o + \frac{d_g}{2} + \frac{d_p}{2})$, and constraint g6 becomes:

g6: $\left(0.68 - (r_o + \frac{d_g}{2} + \frac{d_p}{2})\right) - R \leq 0$

The other constraints remain unchanged and are also constraints for the system.

6.2.2 Gear Constraint Updates

When optimizing the gear as a subsystem, there were several variables that interacted with the other subsystems in order to give a subsystem optimal. The constraints are updated to reflect these variables. Additionally, the constraints are updated to be in terms of meters instead of millimeters.

The torque to be transmitted was considered to be a subsystem and the gears were designed for this torque. For the system, this becomes a variable that interacts with the wheels and the shaft. The equations for constraints 1 and 2 for the gear sub system change to the form as given below.

$$K_b = 0.57T_{req}$$

Where T_{req} is the torque required to move the wheel. This T_{req} is calculated using the coefficient of friction, weight of the wheelchair, and the radius of the wheel. The constraints now change to:

g1: $K_b P_d - 106 d_g b \leq 0$

g2: $GR * K_b P_d - 106 d_g b \leq 0$

The constraint that involves the face width was changed as it now had to take into account the length of the shaft in its first step i.e. L1 and the bearing length. However writing this constraint as a part of the system would make it redundant as this constraint will be covered in the shaft subsystem (for the system level constraints).

The entire system is now being optimized for a gear ratio of 2 and sum of pitch circle diameters 0.3m.

An important note in this system optimization is that when the fatigue life factor (C_{Li}^{2}) was calculated, a torque that was considered was double the torque required to move the wheel. When it was found that the actual torque required was only half the design torque, the value of C_{Li}^{2} was halved for the system level optimization.

For the gear subsystem, the torque is the linking variable. The sum of the PCD is constrained as they cannot be bigger than the wheel and the face width as it cannot take more space than what is available for it, after housing the bearing on the first step of the shaft.

6.2.3 Shaft Constraint Updates

For the shaft subsystem the following parameters became variables: (i) wheel diameter, (ii) diameter of the gear, (iii) face width of the gear, and (iv) thickness of the rim.

The wheel diameter was assumed to 600mm, thus the load torque acting on the shaft was assumed to be 150000 Nmm. For system level optimization the diameter of the wheel is a variable, thus the torque acting on the shaft is given by $T=1001*r_o$.

In the system optimization the parameter for diameter of the gear changes from 40mm to 60mm. The face width of the gear becomes a variable, b, and the thickness of the rim becomes a variable t_r. Additionally, constraints were put in terms of meters instead of millimeters.

With these new considerations the constraints for the shaft subsystem are updated for the system optimization in the following ways:

$$g1\text{: } \frac{5.09\sqrt{113.2096 * 10^6 * 2 * L1 + 140906(2r_o)^2}}{d1^3} - 94.5 \times 10^6 \leq 0$$

$$g2\text{:} \frac{2r_o L1^3}{d_g d1^4} - 16.18 \times 10^3 \leq 0$$

$$g3\text{: } \frac{2r_o L1^2}{d_g d1^4} - 5648.424 \leq 0$$

$$g8\text{: } 0.001 + b - L1 \leq 0$$

$$g9\text{: } 0.01 + t_r - L3 \leq 0$$

6.2.4 Wheel Constraint Updates

For the wheel, the following parameters became variables: (i) the radius of the shaft, (ii) the width of the other elements in the subsystem.

The radius of the shaft was assumed to be 10 mm, but is now taken to be the variable $\frac{d3}{2}$. Similarly, the width allowable for the wheels and the rest of the subsystem was originally assumed to be equally distributed (the wheels took up half the space and the rest of the subsystem took up the rest, now however, the width allowable is distributed among the wheels and the length of the shafts, where the length of the shaft is the variable $L1 + L2 + L3$. The constraint on mechanical advantage now takes into account the mechanical advantage gained by the inclusion of the gears. Finally, the constraints are changed to be in terms of meters instead of millimeters.

With these changes, the constraints update in the following ways:

g4: $1.1(\frac{d3}{2}) - r_h \leq 0$

g5: $2t_r + 2(L1 + L2 + L3) - 0.203 \leq 0$

g7: $7.26d3 - r_o \leq 0$

$$m_w = \rho_a \pi t_r (r_o^2 - r_i^2) + \rho_s 24\pi (r_i - r_h) {r_s}^2 + \rho_a \pi t_r (r_h - \frac{d3}{2})^2$$

6.3 Method

We use an All-in-One optimization; all of the constraints of each subsystem are considered in the model. The objective functions of the gears, shaft and wheel are also taken to be constraints in the model. This leads to a model that contained seventeen variables and 37 constraints. The model was then optimized using Matlab fmincon, following the same algorithm as was used in the lever handle subsystem optimization, because this was also the objective function for the overall system optimization.

6.4 Optimization

Our system had a complicated objective function that was not easy to plot in space. The method we resorted to for getting an optimal was hit and trial. Using this method, we found a feasible point and ran the optimization. The results of the optimization, a wheelchair drive mechanism designed for a 95 percentile male, are:

Variable	Symbol	Optimum
length of lever	R	0.432 m
horizontal displacement of lever from shoulder	X	-0.089 m
length 1 of shaft	L1	0.038 m
length 2 of shaft	L2	0.016 m
length 3 of shaft	L3	0.016 m
diameter 1 of shaft	d1	0.034 m
diameter 2 of shaft	d2	0.037 m
diameter 3 of shaft	d3	0.034 m
outer radius of wheel rim	ro	0.363 m
inner radius of wheel rim	ri	0.101 m
spoke radius	rs	0.002 m
outer radius of wheel hub	rh	0.035 m
thickness of rim and hub	tr	0.006 m
diameter of gear	dg	0.200 m
diameter of pinion	dp	0.100 m

diametric pitch	Pd	720 teeth/m
width of gear	b	0.020 m
Work Done	**W**	**-898 Nm**

When we put all our constraints together in one system, we had difficulty finding a feasible starting point. To solve this problem, we looked at the subsystem optimum values. We fixed the values of our variables to be around these values and then checked whether the constraints were being satisfied. When we found a combination that did, we used this as a starting point and ran the algorithm. At the end of this iteration, we got an optimum, which we checked for feasibility.

We ran the model for a different set of starting points and it did not seem to be robust, giving the optimum function value around the previous optimum(+/- 30 Nm). Out of 3 sets of feasible starting points that were given, 2 sets gave a feasible solution and the other did not give a solution. The model seems to be robust only to specific starting points in the feasible space and not all of them. If the starting point is infeasible, the model breaks down.

6.5 Comparison with Subsystems

In optimizing the entire system we expect to see that the optima of the included subsystems are no longer met. This is because values initially taken to be parameters are now defined as variables, and the four subsystems are competing to fill the same space. After optimizing our system, we found the following changes have taken place in our subsystems:

6.5.1 Lever Handle

Comparing optimum values of variables and objective functions for subsystem level optimization and system level optimization of the lever handle, we found that the length of the lever handle reduced, and the position of the lever changed slightly to be behind the shoulder.

Variables	Subsystem	System
R(m)	0.5743	0.432782574
L2(m)	0.0	-0.088606972

From the above table it seen that the length of the lever has decreased from 57.43 cm to 43.28cm, and the position has changed from 0 to -8.8 cm. The change in lever length is approximately 25% and can be attributed to change in the constraint g6 which stated the height of the armrest above the ground. This height was taken to be 0.8 m in the subsystem analysis but was reduced to 0.68 m in the system analysis to reflect a more real value. The other reason is the inclusion of gears which will automatically reduce the length of the lever. The torque also increases as expected because now we include gears which provide mechanical advantage and increase the work output for the user.

6.5.2 Gears

In the system level optimization, the gear dimensions remained the same as they were designed for this specific torque to move the wheels. Their dimensions also mimic the gear ratio, which was an important factor in providing mechanical advantage. The value of face width, which was active in the sub system problem resulted in a face width of 0.04m, while in the system, gave a reduced value of 0.0265m. This may be because the other constraints involving the face width may have provided a tighter bound.

6.5.3 Shaft

Comparing optimum values of variables and objective functions for subsystem level optimization and system level optimization of the shaft, we found that the overall length of the shaft has decreased, but the diameters of all three sections of the shaft have increased.

Variables	Subsystem	System
L1(m)	0.025	0.038
L2(m)	0.035	0.0165
L3(m)	0.035	0.0165
d1(m)	0.02428	0.0335
d2(m)	0.02671	0.0369
d3(m)	0.02428	0.0335
Volume(m^3)	$6.0379*10^{-5}$	$8.3629*10^{-5}$

From the above table it seen that the diameter of the shaft has increased from 24.28mm to 33.5mm, that is almost 38% , this is mainly because of the changed values of the parameters. Due to changes in the diameters the volume of the shaft also changes from $6.0379*10^{-5}$ to

$8.3629*10^{-5}$, that is almost 38%. The cause for increase in the diameter is that forces and the torque acting on the shaft have increased from the subsystem model to the system model. The length of the shaft decreasing is likely due to it having to fit within the packaging constraints supplied by the wheel subsystem.

6.5.4 Wheel

Comparing optimum values of variables and objective functions for subsystem level optimization and system level optimization of the wheel, we found that the overall size of the wheel has increased.

Variable	Subsystem	System
ro	0.305 m	0.362 m
ri	0.277 m	0.101 m
rs	0.0018 m	0.0017 m
rh	0.114 m	0.035 m
tr	0.0036 m	0.006 m

As seen in the table, there was an increase in the outer radius of the wheel. This is due to the interaction between the height of the wheel and the height of the lever handle. The additional constraints put on the wheel by the lever require it to be larger. Because the wheel got larger the spokes had to compensate due to the constraint on buckling by getting shorter. This causes the inner rim diameter to get smaller, which makes the overall rim thicker.

Interestingly, the wheel optimized in the subsystem reasonably accurately reflects wheels commonly seen on wheelchairs or bicycles, aside from the extreme thinness (tr). Now in the system optimization, the wheel no longer looks like the current design. The difference between ro and ri is too large, and the thinness is still an issue. This suggests that the missing constraints and over-simplifications in the subsystem design have been magnified in the system design, and also that the system design may not accurately represent all of the interactions between the different subsystems.

6.6 Parametric Study

A parametric study was conducted by looking at female users in addition to male users. The results show the maximum work that can be extracted from this system for the 95^{th} percentile male and 95^{th} percentile female by changing their respective arm lengths.

The results from the numerical analysis show that for a 95^{th} percentile male with given arm settings, the maximum work that can be extracted for a given stroke angle is approximately 898 Nm. The respective values of the design variables are given in the attached appendix. The maximum work that can be extracted out of this system for a 95^{th} percentile female was 522 Nm. The main issue in the design space seems to be the behavior of the objective function and the difficulty of getting more feasible starting points.

Variable	Symbol	Optimum for 95% Men	Optimum for 95% Women
length of lever	R	0.432 m	0.413 m
horizontal displacement of lever from shoulder	X	-0.089 m	-0.068 m
length 1 of shaft	L1	0.038 m	0.036 m
length 2 of shaft	L2	0.016 m	0.023 m
length 3 of shaft	L3	0.016 m	0.022 m
diameter 1 of shaft	d1	0.034 m	0.034 m
diameter 2 of shaft	d2	0.037 m	0.061 m
diameter 3 of shaft	d3	0.034 m	0.034 m
outer radius of wheel rim	ro	0.363 m	0.380 m
inner radius of wheel rim	ri	0.101 m	0.141 m
spoke radius	rs	0.002 m	0.003 m
outer radius of wheel hub	rh	0.035 m	0.104 m
thickness of rim and hub	tr	0.006 m	0.006 m
diameter of gear	dg	0.200 m	0.255 m
diameter of pinion	dp	0.100 m	0.045 m
diametric pitch	Pd	720 teeth/m	355 teeth/m
width of gear	b	0.020 m	0.025 m
Work Done	**W**	**-898 Nm**	**-522 Nm**

Here we see that due to the differences in arm length and mass between a woman in the 95 percentile and a man in the 95 percentile, the torque supplied by the user would be less and the wheel would have to become larger, which would then affect all other parts of the system. The work done by the drive mechanism in the case of the woman is significantly lower than that for the man.

6.7 Discussion of Results and Conclusions

The model only converged to the same "optimizer" a few times out of the many feasible starting points that we chose. This may be because the feasible domain is either very small as defined by these constraints or has infeasible holes scattered throughout. A possible reason the domain has scattered infeasible holes is because the objective function is based on an integral and it is a non-constant function. This means that depending upon the initial point given to fmincon, different optimum were given, or no feasible optimum could be found. It is possible that if the bounds on the critical variables of the model were reduced enough, fmincon would not jump into infeasible regions, and convergence could be found.

Appendix A: Measurements of the standard manual wheelchair from the American Disabilities Act

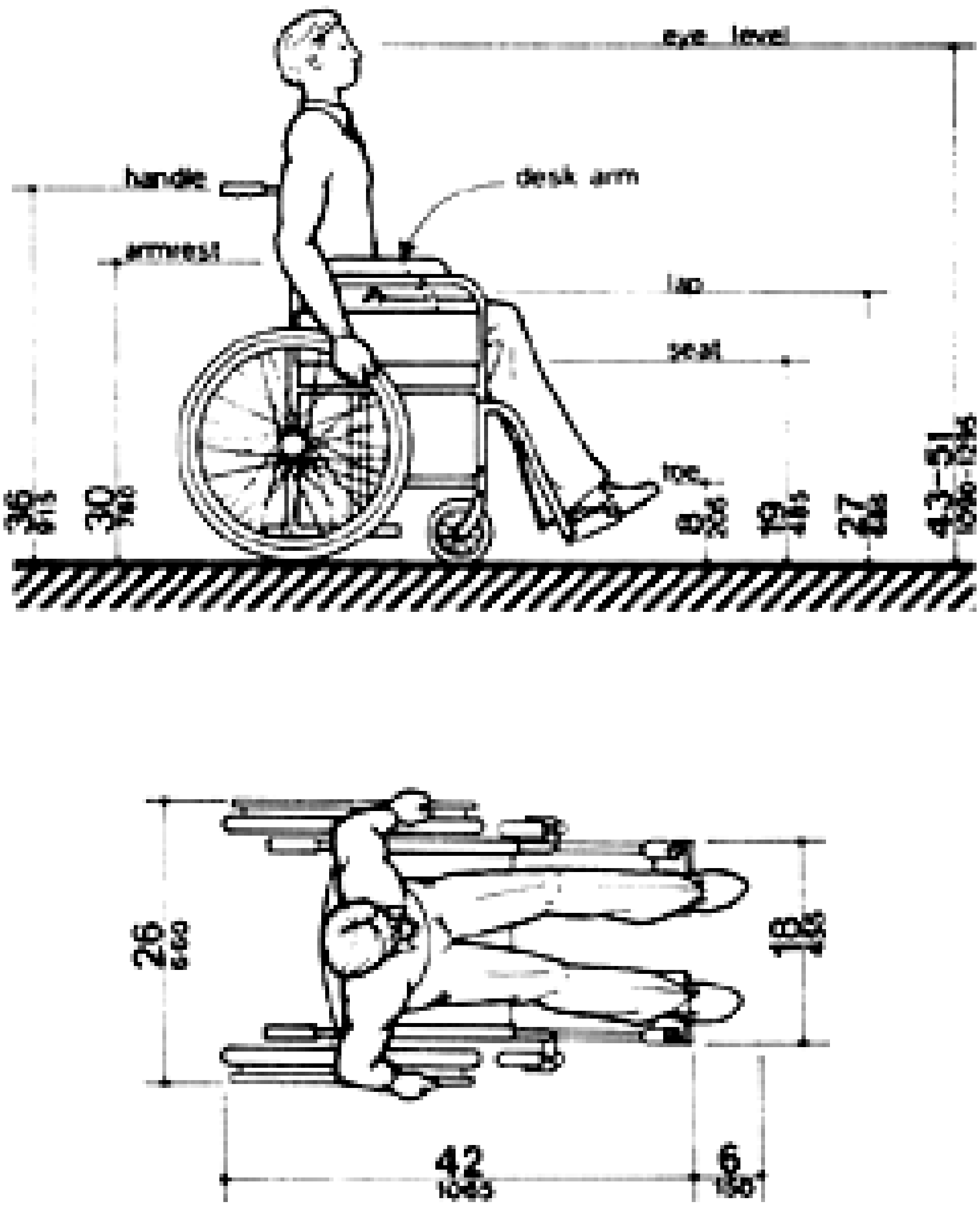

NOTE: Footrests may extend further for tall people

Fig. A3
Dimensions of Adult-Sized Wheelchairs

Appendix B: Convergence for Lever Handle Optimization

(II) Results for 95% male after scaling R and X by a factor of 1000.

SL no	Starting Points		Final Points				KKT Norm	Fval
	R(mm)	X(mm)	Ropt(mm)	Xopt(mm)	Ropt(cm)	Xopt(cm)		
1	500	500	551.3821	-29.3089	55.13821	-2.93089	10^-11	-880.471
2	750	-500	574.2727	0	57.42727	0	0.020557	-880.251
3	6000	-50	573.8272	-18.0864	57.38272	-1.80864	9.077356	-880.853
4	5700	-10	574.4411	-17.7794	57.44411	-1.77794	0.236164	-880.863
5	5750	-15	572.3005	-18.8498	57.23005	-1.88498	11.13015	-880.827

(III) Results for 95% female

SL no	Starting Points		Final Points				KKT norm	fval
	R(m)	X(m)	Ropt(m)	Xopt(m)	Ropt(cm)	Xopt(cm)		
1	0	0	0.57318	2.37E-08	57.31802	2.37E-06	1.45E+02	-511.657
2	0.5	0.5	0.573182	0.000821	57.31818	0.082067	1.92E+02	-511.636
3	0.75	-0.5	0.55	0	55	0	4.11E-15	-511.037
4	1	-1	0.55	0.00E+00	55	0	0.00E+00	-511.037
5	2	1	0.55	0	55	0	0	-511.037
6	5	0	0.573182	1.21E-07	57.31818	1.21E-05	8.09E+01	-511.657
7	10	10	0.573182	0	57.31818	0	2.59E+03	-511.657
8	100	100	0.55	0	55	0	1.96E-12	-511.037
9	100	-200	0.573182	2.67E-07	57.31818	2.67E-05	6.03E-05	-511.657
10	0	-10	0.573182	2.67E-07	57.31818	2.67E-05	2.18E+02	-511.657

Appendix C: fmincon codes for subsystem optimization

1. Lever

Objective function:

```
% clear all;
   function y = modified(xx)
   R = xx(1);
   X = xx(2);
   alpha1=0.3017; %0.1924-females
   alpha2=0.1488; %0.1011-females
   l1=0.323;      %0.295-females
   l2=0.287;      %0.255-females
   m1=2.7524;     %2.2525-females
   m2=2.18226;    %0.1.73893-females
   theta3 = pi/3:pi/18:2*pi/3; %the values of theta3 ranges from 60' to 120
   and I have divided the range into 6 intervals'
   theta = zeros(7,2);torque=zeros(7,1); %possible combination 7 values of
   theta3
   n =1;
   for i=1:length(theta3)
       options=optimset('Display','iter');
       F = @(x)[-l1*cos(x(1)) + l2*sin(x(2)) + R*cos(theta3(i)) + 0.7;
                 l1*sin(x(1)) + l2*cos(x(2)) + R*sin(theta3(i)) - X];
       [x,fval] = fsolve(F,[pi/10 pi/10],options);
       theta(n,:) = x;
       n = n+1;
   end
   %the o/p is 7 values of theta1 and theta1
   for i=1:7
       torque(i,1)=alpha1*(227.338+0.525*theta(i,2)-
   .296*theta(i,1))+alpha2*(336.29+1.544*theta(i,2)-.085*(theta(i,2))^2-
   0.5*(theta(i,1)))-((m1+m2)*9.8143*sin(theta(i,1))*l1/2)-
   (m2*9.8143*cos(pi/2+theta(i,1)-theta(i,2))*l2/2);
       %finding torque values for each theta1 and theta2 thus total 7
   different torques for 7 values of theta1 and theta2
   end
   y =-sum(torque);
```

Constraints:

```
   function [g,h]=NONLCON1(xx)
   % inequality constraints
   l1=0.323;      %0.295-females
   l2=0.287;      %0.255-females
   R=xx(1);X=xx(2);
   g=[   1.1*R+1.1*l1-l2-sqrt(X^2+0.7^2);
         0.45-R;
         -xx(2);
         X+R*cos(pi/3)-(l1+l2);
      ];

   % equality constraints
   h=[];
```

```
end


function [g,h]=NONLCON2(xx)
% inequality constraints
l1=0.323;      %0.295-females
l2=0.287;      %0.255-females
R=xx(1);X=xx(2);
g=[   1.1*R+1.1*l1-l2-sqrt(X^2+0.7^2);
      0.45-R;
      xx(2)
      -R*cos(2*pi/3)-X-(l1+l2)*cos(pi/3);
    ];

% equality constraints
h=[];
end
```

Optimizer:

```
clc;
clear all;
OPTIONS = optimset('Algorithm','interior-point');
A=[ ]; b=[ ]; Aeq=[ ]; beq=[ ]; % matrix/vectors for defining linear
constraints (not used)
lb = [0,0]; % lower bounds on the problem
ub = [ ]; % upper bounds on the problem (not used)
ip=[100,-200];
[xopt1,fval1,exitflag1,ouput1,lambda1,grad1,hessian1]=
fmincon('modified',ip,A,b,Aeq,beq,lb,ub,'NONLCON1');
[xopt2,fval2,exitflag2,ouput2,lambda2,grad2,hessian2]=
fmincon('modified',ip,A,b,Aeq,beq,[0,-Inf],[Inf,0],'NONLCON2');
if(fval1<fval2)
xopt=xopt1;fval=fval1;ouput=ouput1;
else
xopt=xopt2;fval=fval2;ouput=ouput2;
end
```

2. Gears

Function:

```
function [ f ] = FUN( x )
% This function is for the fatigue life of the gear
Ks = 9*10^12;
f =((Ks/x(4)) * ((1/x(2)^2) + (1/(x(1)*x(2)))));
end
```

Constraints:

```
function [ g,h ] = NONLCON( x )
% Inequality constraints

Kb = 1.5 * 10^5;
GR = 3;
```

```
g=[
Kb * x(3) - 106 * x(1) * x(4);
GR * Kb * x(3) - 106 * x(1) * x(4);
16 - x(3) * x(2);
16 - x(3) * x(1);
9 - x(3) * x(4);
x(3) * x(4) - 14;
x(4) - 40;
GR * x(2) - x(1);
x(1) * x(3) - (0.085 * (x(3))^2 * x(2)*(2 * x(1) + x(2)) + 1);
x(1) + x(2) - 250;
];

% Equality constraints
h = [];
end
```

Optimizer:

```
clear all;
clc;
OPTIONS = optimset('Algorithm', ‘sqp','MaxIter',10000,'TolCon',1e-06,
'TolFun',1e-06);
A = []; b = []; Aeq = []; beq = []; % Vectors defining the linear constraints
lb = [50,50,0,0]; % Lower bounds of the design variables
ub = [];          % Upper bounds of the design variables

[xopt,fval,exitflag,lamda,ouput,HESSIAN] =
fmincon('FUN',[190,60,0.4,30],A,b,Aeq,beq,lb,ub,'NONLCON');

%,xopt = fmincon('FUN',x0,A,b,Aeq,beq,lb,ub,'NONLCON');

x=xopt;

Kb = 1.5 * 10^5;
Ks = 9*10^12;
GR = 3;

g=[
Kb * x(3) - 106 * x(1) * x(4);
GR * Kb * x(3) - 106 * x(1) * x(4);
16 - x(3) * x(2);
16 -  x(3) * x(1);
9 -  x(3) * x(4);
x(3) * x(4) - 14;
x(4) - 40;
GR * x(2) - x(1);
x(1) * x(3) - (0.085 * (x(3))^2 * x(2)*(2 * x(1) + x(2)) + 1);
x(1) + x(2) - 250;
];
```

3. Shaft

Objective function:

```
function [f]=FUN(x)
% the percent sign allows me to write in comments
f= x(1)*x(4)^2+x(2)*x(5)^2+ x(3)*x(6)^2 ;
end
```

Constraints:

```
function [g,h]=NONLCON(x)
% inequality constraints
g=[ ((5.09*sqrt((113.2096*10^6*x(1)^2)+(5.0625^10)))/x(4)^3)-182.25;
          (x(1)^3/x(4)^4)-16.18;
          (x(1)^2/x(4)^4)-5.2359*10^-3;
          1.1*x(4)-x(5);
          1.1*x(6)-x(5);
          x(1)+x(2)+x(3)-130;
          25-x(1);
          35-x(3);
          x(3)-x(2);
          x(4)-x(6);
          3-x(4);
          3-x(5);
         3-x(6);
         ];
      % equality constraints
      h=[ ];
      end
```

Optimizer:

```
clc;clear all;
OPTIONS = optimset('Algorithm','interior-point');
A=[ ]; b=[ ]; % matrix/vectors for defining linearconstraints (notused)
Aeq=[ ]; beq=[ ];
lb = [0,0,0,0,0,0];            % lower bounds on the problem
ub = [ ];                      % upper bounds on the problem (not used)
[xopt,fval,exitflag,ouput] =
fmincon('FUN',[1,1,1,1,1,1],A,b,Aeq,beq,lb,ub,'NONLCON');
```

4. Wheel

Objective Function:

```
function [f]=fun5(x);
f=(2.7e-6*pi*x(1)*(x(2)^2-x(3)^2))+(8e-6*24*pi*(x(3)-x(4))*x(5)^2)+(2.7e-
6*pi*x(1)*(x(4)-10)^2);
end
```

Nonlinear Constraints:

```
function [c,ceq]=nonlcon5(x)
%nonlinear inequality constraints
c=[(1.5*9.81*(146+2*((2.7e-6*pi*x(1)*(x(2)^2-x(3)^2))+(8e-6*24*pi*(x(3)-
x(4))*x(5)^2)+(2.7e-6*pi*x(1)*(x(4)-
10)^2)))*cos(pi/4))/(2*x(2)*x(1)*sin(pi/8))-55;
    (1.5*9.81*(146+2*((2.7e-6*pi*x(1)*(x(2)^2-x(3)^2))+(8e-6*24*pi*(x(3)-
x(4))*x(5)^2)+(2.7e-6*pi*x(1)*(x(4)-10)^2)))-
((pi^3*193e3*x(5)^4)/(4*(0.5*(x(3)-x(4)))^2)))];
ceq=[];
end
```

Linear Constraints and Optimizer

```
clear all
options=optimset('Algorithm','sqp','Display','iter','LargeScale','off');

A=[0 1 0 0 0;
    0 0 -1 1.1 0;
    0 -1 1.1 0 0;
    0 0 0 -1 0;
    4 0 0 0 0;
    -1 0 0 0 2;
    0 -1 0 0 0;
    0 0 0 -2*pi 48;];
b=[380;
    0;
    0;
    -11;
    203;
    0;
    -305;
    0;];
Aeq=[];beq=[];
lb=[0,0,0,0,0];
ub=[];
x0=[90,58,522,27,5];

[xopt,fval,exitflag,output]=fmincon('fun5',x0,A,b,Aeq,beq,lb,ub,'NONLCON5')
```

Appendix D: fmincon codes for System Optimization

Optimizer

```
tic;clc;
clear all;
alpha1=0.3017; %0.1924-females
alpha2=0.1488; %0.1011-females
l1=0.323;      %0.295-females
l2=0.287;      %0.255-females
m1=2.7524;     %2.2525-females
m2=2.18226;    %0.1.73893-females
GR=2;
Ks=3*10e+09;
OPTIONS = optimset('Algorithm','interior-point');
A=[ ]; b=[ ]; Aeq=[ ]; beq=[ ]; % matrix/vectors for defining linear
constraints (not used)
lb = [0,0]; % lower bounds on the problem
ub = [ ]; % upper bounds on the problem (not used)
%R=0.38;X=0;L1=0.025;L2=0.035;L3=0.035;d1=0.242;d2=0.267;d3=0.242;ro=.305;ri=
0.27;rs=0.0019;rh=0.135;tr=0.0038;dg=0.200;dp=0.100;Pd=342.9;b=0.040;
ip=[0.432782574 -0.088606972    0.038006415 0.016478973 0.016478973 0.033522
0.0368742   0.033522    0.362900334 0.101473996 0.001699503 0.035134562
0.006478973 0.199999148 0.099998085 729.7228345 0.019185366

];
%R=xx(1);X=xx(2);L1=xx(3);L2=xx(4);L3=xx(5);d1=xx(6);d2=xx(7);d3=xx(8);ro=x
%x(9);ri=xx(10);rs=xx(11);rh=xx(12);tr=xx(13);dg=xx(14);dp=xx(15);Pd=xx(16);b
=xx(17);
[xopt1,fval1,exitflag1,ouput1,lambda1,grad1,hessian1]=
fmincon('modified',ip,A,b,Aeq,beq,lb,ub,'NONLCON1');
[xopt2,fval2,exitflag2,ouput2,lambda2,grad2,hessian2]=
fmincon('modified',ip,A,b,Aeq,beq,[0,-Inf],[Inf,0],'NONLCON2');
if(fval1<fval2)
    xopt=xopt1;fval=fval1;ouput=ouput1;
else
    xopt=xopt2;fval=fval2;ouput=ouput2;
end

R=xopt1(1);X=xopt1(2);L1=xopt1(3);L2=xopt1(4);L3=xopt1(5);d1=xopt1(6);d2=xopt
1(7);d3=xopt1(8);ro=xopt1(9);ri=xopt1(10);rs=xopt1(11);rh=xopt1(12);tr=xopt1(
13);dg=xopt1(14);dp=xopt1(15);Pd=xopt1(16);b=xopt1(17);
    constarint1=[1.1*R+1.1*l1-l2-sqrt(X^2+(1.05-(ro+(dg+dp/2)))^2);
    0.68-ro-(R+(dp+dg)/2);
    -X;
    X+R*cos(pi/3)-(l1+l2);
    ro-0.380;
    1.1*rh-ri;
    1.1*ri-ro;
    1.1*(d3/2)-rh;
    2*tr+2*(L1+L2+L3)-0.203;
    7.62*d3-ro;
    48*rs-2*pi*rh;
    2*rs-tr;
    (0.75*9.81*(146+2*((2.7e3*pi*tr*ro^2-ri)^2))+(8e3*24*pi*(ri-
rh)*rs^2)+(2.7e3*pi*tr*rh-(d3/2)^2))*cos(pi/4)/(2*ro*tr*sin(pi/8))-55e6;
```

```
    (0.75*9.81*(146+2*(2.7e3*pi*tr*ro^2-ri^2))+(8e3*24*pi*(ri-
rh)*rs^2)+(2.7e3*pi*tr*rh-(d3/2)^2))-((pi^3*193e9*rs^4)/(4*(0.5*ri-rh))^2);
   ((5.09*sqrt((113.2096e6*L1^2)+(140906*(2*ro)^2)))/d1^3)-94.5e6;
    (((2*ro)*L1^3)/(dg*d1^4))-16.18e3;
    (((2*ro)*L1^2)/(dg*d1^4))-5648.71;
    1.1*d1-d2;
    1.1*d3-d2;
    L1+L2+L3-.130;
    0.010+b-L1;
    0.010+tr-L3;
    L3-L2;
    d1-d3;
    0.003-d1;
    0.003-d2;
    0.003-d3;
    (0.57*0.7*((146*9.81)/2)*ro)*Pd-106.575e6*dg*b;
    GR*(0.57*0.7*((146*9.81)/2)*ro)*Pd-106.575e6*dp*b;
    16-dp*Pd;
    16-dg*Pd;
    9-Pd*b;
    Pd*b-14;
    GR*dp-dg;
    dg*Pd-0.085*dp*Pd^2*(2*dg+dp+1);
    dg+dp-0.300;
    6.0379*10^-5-(pi/4*(d1^2*L1+d2^2*L2+d3^2*L3));
    0.88-((2.7e3*pi*tr*(ro^2-ri)^2)+(8e3*24*pi*(ri-rh)*rs^2)+(2.7e3*pi*tr*rh-
(d3/2)^2));
    (1.35*10e+13)/2- (Ks/b)*((1/(dp^2))+(1/(dp*dg)));
    ];

R=xopt2(1);X=xopt2(2);L1=xopt2(3);L2=xopt2(4);L3=xopt2(5);d1=xopt2(6);d2=xopt
2(7);d3=xopt2(8);ro=xopt2(9);ri=xopt2(10);rs=xopt2(11);rh=xopt2(12);tr=xopt2(
13);dg=xopt2(14);dp=xopt2(15);Pd=xopt2(16);b=xopt2(17);
    constarint2=[1.1*R+1.1*l1-l2-sqrt(X^2+(1.05-(ro+(dg+dp)/2))^2);
    0.68-ro-(R+(dp+dg)/2);
     X;
    -R*cos(2*pi/3)-X-(l1+l2)*cos(pi/3);
    ro-0.380;
    1.1*rh-ri;
    1.1*ri-ro;
    1.1*(d3/2)-rh;
    2*tr+2*(L1+L2+L3)-0.203;
    7.62*d3-ro;
    48*rs-2*pi*rh;
    2*rs-tr;
    (0.75*9.81*146+2*((2.7e3*pi*tr*ro^2-ri)^2))+(8e3*24*pi*(ri-
rh)*rs^2)+(2.7e3*pi*tr*rh-(d3/2)^2)*cos(pi/4)/(2*ro*tr*sin(pi/8))-55e6;
    (0.75*9.81*146+2*(2.7e3*pi*tr*ro^2-ri^2))+(8e3*24*pi*(ri-
rh)*rs^2)+(2.7e3*pi*tr*rh-(d3/2)^2)-((pi^3*193e9*rs^4)/(4*(0.5*ri-rh))^2);
   ((5.09*sqrt((113.2096e6*L1^2)+(140906*(2*ro)^2)))/d1^3)-94.5e6;
    (((2*ro)*L1^3)/(dg*d1^4))-16.18e3;
    (((2*ro)*L1^2)/(dg*d1^4))-5648.71;
    1.1*d1-d2;
    1.1*d3-d2;
    L1+L2+L3-.130;
    0.010+b-L1;
    0.010+tr-L3;
```

```
    L3-L2;
    d1-d3;
    0.003-d1;
    0.003-d2;
    0.003-d3;
    (0.57*0.7*((146*9.81)/2)*ro)*Pd-106.575e6*dg*b;
    GR*(0.57*0.7*((146*9.81)/2)*ro)*Pd-106.575e6*dp*b;
    16-dp*Pd;
    16-dg*Pd;
    9-Pd*b;
    Pd*b-14;
    GR*dp-dg;
    dg*Pd-0.085*dp*Pd^2*(2*dg+dp+1);
    dg+dp-0.300;
    6.0379*10^-5-(pi/4*(d1^2*L1+d2^2*L2+d3^2*L3));
    0.88-((2.7e3*pi*tr*(ro^2-ri)^2)+(8e3*24*pi*(ri-rh)*rs^2)+(2.7e3*pi*tr*rh-
(d3/2)^2));
    (1.35*10e+13)/2- (Ks/b)*((1/(dp^2))+(1/(dp*dg)));
    ];
toc;
```

Constraints

Nonlcon 1

```
function [g,h]=NONLCON1(xx)
% inequality constraints
l1=0.323;       %0.295-females
l2=0.287;       %0.255-females
R=xx(1);X=xx(2);L1=xx(3);L2=xx(4);L3=xx(5);d1=xx(6);d2=xx(7);d3=xx(8);ro=xx(9
);ri=xx(10);rs=xx(11);rh=xx(12);tr=xx(13);dg=xx(14);dp=xx(15);Pd=xx(16);b=xx(
17);
GR=2;
Ks=3*10e+09;
g= [
    1.1*R+1.1*l1-l2-sqrt(X^2+(1.05-(ro+(dg+dp/2)))^2);
    0.68-ro-(R+(dp+dg)/2);
    -X;
    X+R*cos(pi/3)-(l1+l2);
    ro-0.380;
    1.1*rh-ri;
    1.1*ri-ro;
    1.1*(d3/2)-rh;
    2*tr+2*(L1+L2+L3)-0.203;
    7.62*d3-ro;
    48*rs-2*pi*rh;
    2*rs-tr;
    (0.75*9.81*(146+2*((2.7e3*pi*tr*ro^2-ri)^2))+(8e3*24*pi*(ri-
rh)*rs^2)+(2.7e3*pi*tr*rh-(d3/2)^2))*cos(pi/4)/(2*ro*tr*sin(pi/8))-55e6;
    (0.75*9.81*(146+2*(2.7e3*pi*tr*ro^2-ri^2))+(8e3*24*pi*(ri-
rh)*rs^2)+(2.7e3*pi*tr*rh-(d3/2)^2))-((pi^3*193e9*rs^4)/(4*(0.5*ri-rh))^2);
   ((5.09*sqrt((113.2096e6*L1^2)+(140906*(2*ro)^2)))/d1^3)-94.5e6;
    (((2*ro)*L1^3)/(dg*d1^4))-16.18e3;
    (((2*ro)*L1^2)/(dg*d1^4))-5648.71;
    1.1*d1-d2;
    1.1*d3-d2;
    L1+L2+L3-.130;
    0.010+b-L1;
```

```
    0.010+tr-L3;
    L3-L2;
    d1-d3;
    0.003-d1;
    0.003-d2;
    0.003-d3;
    (0.57*0.7*((146*9.81)/2)*ro)*Pd-106.575e6*dg*b;
    GR*(0.57*0.7*((146*9.81)/2)*ro)*Pd-106.575e6*dp*b;
    16-dp*Pd;
    16-dg*Pd;
    9-Pd*b;
    Pd*b-14;
    GR*dp-dg;
    dg*Pd-0.085*dp*Pd^2*(2*dg+dp+1);
    dg+dp-0.300;
    d3-.75*dp;
   6.0379*10^-5-(pi/4*(d1^2*L1+d2^2*L2+d3^2*L3));
   0.88-((2.7e3*pi*tr*(ro^2-ri)^2)+(8e3*24*pi*(ri-rh)*rs^2)+(2.7e3*pi*tr*rh-
(d3/2)^2));
    (1.35*10e+13)/2- (Ks/b)*((1/(dp^2))+(1/(dp*dg)));
    ];
% equality constraints
h=[];


end
```

Nonlcon 2

```
function [g,h]=NONLCON2(xx)
% inequality constraints
l1=0.323;      %0.295-females
l2=0.287;      %0.255-females
R=xx(1);X=xx(2);L1=xx(3);L2=xx(4);L3=xx(5);d1=xx(6);d2=xx(7);d3=xx(8);ro=xx(9
);ri=xx(10);rs=xx(11);rh=xx(12);tr=xx(13);dg=xx(14);dp=xx(15);Pd=xx(16);b=xx(
17);
GR=2;
Ks=3*10e+09;
g= [
    1.1*R+1.1*l1-l2-sqrt(X^2+(1.05-(ro+(dg+dp)/2))^2);
    0.68-ro-(R+(dp+dg)/2);
     X;
    -R*cos(2*pi/3)-X-(l1+l2)*cos(pi/3);
    ro-0.380;
    1.1*rh-ri;
    1.1*ri-ro;
    1.1*(d3/2)-rh;
    2*tr+2*(L1+L2+L3)-0.203;
    7.62*d3-ro;
    48*rs-2*pi*rh;
    2*rs-tr;
    (0.75*9.81*(146+2*((2.7e3*pi*tr*(ro^2-ri)^2)+(8e3*24*pi*(ri-
rh)*rs^2)+(2.7e3*pi*tr*rh-(d3/2)^2)))*cos(pi/4))/(2*ro*tr*sin(pi/8))-55e6;
    (0.75*9.81*(146+2*(2.7e3*pi*tr*(ro^2-ri^2))+(8e3*24*pi*(ri-
rh)*rs^2)+(2.7e3*pi*tr*rh-(d3/2)^2))-((pi^3*193e9*rs^4)/(4*(0.5*ri-rh))^2));
   ((5.09*sqrt((113.2096e6*L1^2)+(140906*(2*ro)^2)))/d1^3)-94.5e6;
    (((2*ro)*L1^3)/(dg*d1^4))-16.18e3;
```

```
    (((2*ro)*L1^2)/(dg*d1^4))-5648.71;
    1.1*d1-d2;
    1.1*d3-d2;
    L1+L2+L3-.130;
    0.010+b-L1;
    0.010+tr-L3;
    L3-L2;
    d1-d3;
    0.003-d1;
    0.003-d2;
    0.003-d3;
    (0.57*0.7*((146*9.81)/2)*ro)*Pd-106.575e6*dg*b;
    GR*(0.57*0.7*((146*9.81)/2)*ro)*Pd-106.575e6*dp*b;
    16-dp*Pd;
    16-dg*Pd;
    9-Pd*b;
    Pd*b-14;
    GR*dp-dg;
    dg*Pd-0.085*dp*Pd^2*(2*dg+dp+1);
    dg+dp-0.300;
   d3-.75*dp;
    6.0379*10^-5-(pi/4*(d1^2*L1+d2^2*L2+d3^2*L3));
    0.88-((2.7e3*pi*tr*(ro^2-ri)^2)+(8e3*24*pi*(ri-rh)*rs^2)+(2.7e3*pi*tr*rh-
(d3/2)^2));
    (1.35*10e+13)/2- (Ks/b)*((1/(dp^2))+(1/(dp*dg)));
    ];

% equality constraints
h=[];


end
```

Modified

```
% clear all;
function y = modified(xx)
R=xx(1);X=xx(2);L1=xx(3);L2=xx(4);L3=xx(5);d1=xx(6);d2=xx(7);d3=xx(8);ro=xx(9
);ri=xx(10);rs=xx(11);rh=xx(12);tr=xx(13);dg=xx(14);dp=xx(15);Pd=xx(16);b=xx(
17);
alpha1=0.3017; %0.1924-females
alpha2=0.1488; %0.1011-females
l1=0.323;      %0.295-females
l2=0.287;      %0.255-females
m1=2.7524;     %2.2525-females
m2=2.18226;    %0.1.73893-females
theta3 = pi/3:pi/18:2*pi/3; %the values of theta3 ranges from 60' to 120 and
I have divided the range into 6 intervals'
theta = zeros(7,2);torque=zeros(7,1); %possible combination 7 values of
theta3
n =1;
for i=1:length(theta3)
    options=optimset('Display','iter');
    F = @(x)[-l1*cos(x(1)) + l2*sin(x(2)) + R*cos(theta3(i)) - (1.05-
(ro+(dg+dp)/2));
              l1*sin(x(1)) + l2*cos(x(2)) + R*sin(theta3(i)) - X];
    [x,fval] = fsolve(F,[pi/10 pi/10],options);
```

```
    theta(n,:) = x;
    n = n+1;
end
%the o/p is 7 values of theta1 and theta1
for i=1:7
    torque(i,1)=alpha1*(227.338+0.525*theta(i,2)-
.296*theta(i,1))+alpha2*(336.29+1.544*theta(i,2)-.085*(theta(i,2))^2-
0.5*(theta(i,1)))-((m1+m2)*9.8143*sin(theta(i,1))*l1/2)-
(m2*9.8143*cos(pi/2+theta(i,1)-theta(i,2))*l2/2);
    %finding torque values for each theta1 and theta2 thus total 7 different
torques for 7 values of theta1 and theta2
end
y =-sum(torque);
```

Works Cited

1. **Krishnana, Anjan Kumar, Sriram Narayanan, Akshay Aggarwal and Perwez Akjtar.** *Design of a Wheelchair.* 2010.

2. **Chaffin, Don B. and Gunnar B.J. Anderson.** *Occupational Biomechanics.*

3. **Armstrong, Thomas J.** *Biomechanical Aspects of Hand Work: Anthropometry.*

4. **Bui, Khanh D. and Warren S. Jocz.** *Optimization of Upper Body Work Ouytput for Wheelchair Applications.*

5. [Online] http://www.softintegration.com/chhtml/toolkit/mechanism/fourbar/fourbarNonGrashof.html.

6. **ADA.** PART 36 -- NONDISCRIMINATION ON THE BASIS OF DISABILITY BY PUBLIC ACCOMMODATIONS AND IN COMMERCIAL FACILITIES. *American Disabilities Act.* [Online] 2010. http://www.ada.gov/reg3a.html#anchor03.

7. **Chairs, Melrose.** Wheels. *Merose Kiwi Concept Chairs USA.* [Online] 2011. http://www.melrosewheelchairs.com/index.php?main_page=index&cPath=8_2.

8. **Brandt, Jobst.** *The Bicycle Wheel, 3rd Edition.* Palo Alto : Avocet, Inc.

9. **Hartz, Andrew D.** *FInite Element Analysis of the Classic Bicycle Wheel.* Indianapolis : Rose-Hulman Institute of Technology, 2002.

10. **Drescher, J.P Hambleton and A.** *On modeling a rolling wheel in the presence of plastic deformation as a three- or two-dimensional process.* Minneapolis : Dept of Civil Engineering, University of Minnesota.

11. **Halls, Steven B.** Men's Weight Chart. *Halls MD.* [Online] 200. http://www.halls.md/chart/men-weight-w.htm.

12. **ASM.** Aluminum 6061-O. *Aerospace Specification Metals, Inc.* [Online] http://asm.matweb.com/search/SpecificMaterial.asp?bassnum=MA6061O.

13. **AZoM.** Stainless Steel Grade 304. *AZO Materials.* [Online] 2011. http://www.azom.com/Details.asp?ArticleID=965#_Mechanical_Properties.

14. **Shigley, Joseph Edward.** *Theory of Machines.*

15. **Lingaiah, K.** *Machine Design Databook 2nd Edition.*

16. **Sharma, P.C. and D.K. Agarwal.** *Machine Design.*

17. **Kalpakjian, S. and S. R. Schmid.** *Manufacturing Processes for Engineering Materials Fourth Edition.* 2003.